Laboratório de Implantação Iônica
Instituto de Física – UFRGS

40 anos

Ion Implantation Laboratory
Institute of Physics - UFRGS



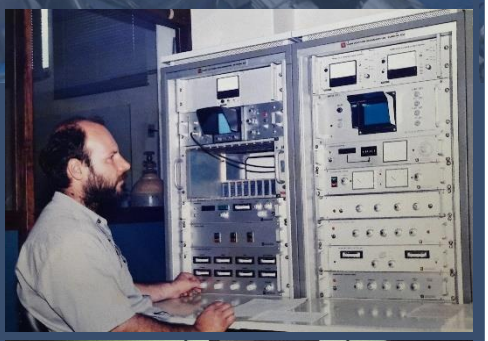




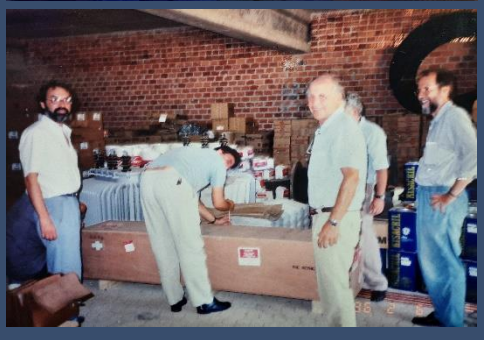


Biennial Report 2021/22

Laboratório de Implantação Iônica

Instituto de Física – UFRGS

Ion Implantation Laboratory

Institute of Physics – UFRGS

Biennial Report – 2021/22

Editors

Henrique Trombini
Silma Alberton Corrêa
Pedro Luis Grande

Porto Alegre

UFRGS IF LABORATÓRIO DE IMPLANTAÇÃO IÔNICA
2023

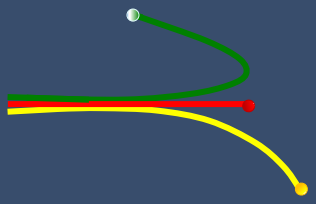

Laboratório de Implantação Iônica
Instituto de Física – UFRGS

Ion Implantation Laboratory
Institute of Physics - UFRGS

Biennial Report 2021/22

Editores:

Henrique Trombini - docente da Universidade Federal de Ciências da Saúde de Porto Alegre (UFCSPA).

Silma Alberton Corrêa - docente da Universidade Federal do Rio Grande do Sul (UFRGS) do Instituto de Química, no Departamento de Físico-Química.

Pedro Luis Grande - docente da Universidade Federal do Rio Grande do Sul (UFRGS) do Instituto de Física, no Departamento de Física.

Dados Internacionais de Catalogação na Publicação (CIP)

Setor Técnico da Biblioteca Professora Ruth de Souza Schneider

Instituto de Física/UFRGS

B588 Biennial Report – 2021/22 [recurso eletrônico] / editado por Henrique Trombini, Silma Alberton Côrrea, Pedro Luis Grande. – Porto Alegre : Laboratório de Implantação Iônica/UFRGS, 2023.
73 p. : il.

ISBN 978-65-5973-331-6

1. Física. 2. Implantação de íons. 3. Análises por feixes de íons. I. Trombini, Henrique. II. Côrrea, Silma Alberton. III. Grande, Pedro Luis. IV. Título.

PACS 61.72

Esse livro está disponível apenas em versão digital no site do Laboratório de Implantação Iônica do Instituto de Física da UFRGS. No endereço eletrônico: http://www.if.ufrgs.br/~grande/arep2022.pdf.

Table of Contents

Preface

The Ion Implantation Laboratory (IIL) is an ion beam center at the Institute of Physics (IF) at the Federal University of Rio Grande do Sul (UFRGS), Brazil. The IF-UFRGS is located in the city of Porto Alegre (state of Rio Grande do Sul) and it is ranked as the most important research center of Physics in southern Brazil.

The IIL has three accelerators that provide a wide variety of positive ions in a broad energy range and are used by tens of researchers from Brazil and other countries from Latin America for ion-beam analysis, ion implantation and ion irradiation. Several beam lines with different analytical techniques are available to scientists from different fields. The techniques are:

PIXE (Particle-Induced X-ray Emission): provides elemental concentrations of the order of part per million;

RBS (Rutherford Backscattering Spectrometry): used for characterization of different structures, including multi-layered targets;

NRA (Nuclear Reaction Analysis) and NRP (Nuclear Reaction Profiling): ideal to detect and profile specific isotopes respectively;

Microprobe: allows the use of techniques like PIXE, RBS and STIM (Scanning Transmission Ion Microscopy) with micrometer beam size;

MEIS (Medium Energy Ion Scattering): it is a high-resolution RBS technique with isotope-separation capability;

ERDA (Elastic Recoil Detection Analysis): for quantitative analysis of light elements in solids, usually H and He;

MeV-SIMS (Secondary Ion Mass Spectrometry induced by MeV ions): used for qualitative molecular analysis;

Ion Implantation: used for modification of materials under controlled parameters.

The infrastructure of the laboratory includes a large variety of ovens, a cleaning room, and a photoluminescence laboratory. A fully dedicated workshop allows the maintenance of the laboratory regularly. A general view of the laboratory is shown below, featuring the beamlines of the Tandetron accelerator.

This book is the eighth issue of our activities and covers two years (2021-2022) of scientific production of all staff members, postdocs, and students of the IIL. Our production was impacted by the pandemic, with our lab being closed for several months, coupled with a reduced number of undergraduate and graduate students. Although there was an increase in the number of students and conferences attended in 2022, the activities in our lab remain lower than pre-pandemic levels. However, we are fully committed to moving forward and enhancing our efforts.

Pedro L. Grande

Head of Ion Implantation Laboratory

Staff

Permanent Researchers

Pedro Luís Grande, PhD. (IF, UFRGS, 1989) - Group leader since 2009.

Johnny Ferraz Dias, PhD. (UG, BELGIUM, 1994) – Accelerators' coordinator since 2010.

Livio Amaral, PhD. (IF, UFRGS, 1982)

Paulo Fernando Papaleo Fichtner, PhD. (IF, UFRGS, 1987)

Henri Ivanov Boudinov, PhD. (IE-BAN, BULGARY, 1991)

Fernanda Chiarello Stedile, PhD. (IQ, UFRGS, 1994)

Ricardo Meurer Papaléo, PhD. (U. UPPSALA, SWEDEN, 1996) PUC-RS

Rogério Luis Maltez, PhD. (IF, UFRGS, 1997)

Claudio Radtke,PhD. (IF, UFRGS, 2003)

Daniel Lorscheitter Baptista, PhD. (IF, UFRGS, 2003)

Gabriel Viera Soares, PhD. (IF, UFRGS, 2008)

Raul Carlos Fadanelli Filho, PhD. (IF, UFRGS, 2005)

Leandro Langie Araujo, PhD. (IF, UFRGS, 2004)

Raquel Giulian, PhD. (RSPE, ANU, AUSTRALIA, 2009)

Jonder Morais, PhD. (UNICAMP, 1995)

Silma Alberton Corrêa, PhD. (IQ, UFRGS, 2013)

Retired Researchers

Fernando Claudio Zawislak, PhD. (IF, UFRGS, 1967) - Founder and Group leader between 1980 and 2008

Moni Behar, PhD. (UBA, ARGENTINA, 1970) – Accelerators' coordinator between 1982 and 2009

Israel Jacob Rabin Baumvol, PhD. (IF, UFRGS, 1977)

Joel Pereira de Souza, PhD. (IF, UFRGS, 2001)

Permanent Technicians

Agostinho A. Bulla, Electrical Engineer responsible for the accelerators

Edison Valério Nunes Junior, Accelerator support and operation

Leandro Tedesco Rossetto, Accelerator support and operation

Paulo Kovalick, Workshop

Postdocs

Raquel Thomaz

Felipe Ferreira Selau

Louise Patron Etcheverry

Where graduates are now?

Andre Luis Fernandes Cauduro, Postdoctoral Researcher, Sandia National Laboratories, California, USA.

Bárbara Canto, Senior Research Associate, AMO GmbH, Germany.

Agenor Hentz da Silva Junior, Professor Adjunto, Departamento de Física, UFSC, SC.

Carla Eliete Iochims dos Santos, Professor Adjunto, Instituto de Matemática, Estatística e Física, FURG, RS.

Carlos Driemeier, Pesquisador, Centro Nacional de Pesquisa em Energia e Materiais, SP.

Cláudia Telles de Souza, Especialista de Pesquisa e Desenvolvimento, Termolar S.A., RS.

Cláudio Radtke, Professor Associado, Departamento de Física, UFRGS, RS.

Cristiane Marin, Professora, UCS, RS.

Cristiano Krug, Professor Adjunto, Departamento de Física, UFRGS.

Dario Ferreira Sanchez, Beamline Scientist at microXAS, Paul Scherrer Institut - PSI, Switzerland.

Deise Schaefer, Professor Adjunto, Departamento de Física, UFSC, SC.

Douglas Langie da Silva, Professor Adjunto, Departamento de Física, UFPEL, RS.

Eduardo Garcia Ribas, Professor, IFSUL, Charqueadas, RS.

Eduardo Pitthan Filho, Researcher, Department of Physics and Astronomy, Uppsala University, Sweden.

Eliana Aquino Van Etten, Process Quality Engineer, Emerson Automation Solutions, Colorado, USA.

Elisa Brod Oliveira da Rosa, Business Development, CEITEC S.A., RS.

Fabiano Bernardi, Professor Associado, Instituto de Física, UFRGS, RS.

Felipe Kremer, Technician in Electronic Microscopy, Australian National University, Australia.

Felipe Lipp Bregolin, Module Process Engineer, Applied Materials Europe, Germany.

Flávia Ferreira Fernandes, Física Médica, Oncologia D'Or, RJ.

Flávia Piegas Luce, Process Team Leader on Ion Implantation, STMicroelectronics, France.

Gabriel Guterres Marmitt, Afdeling Radiotherapie, Universitair Medisch Centrum Groningen, Netherlands.

Gabriel Vieira Soares, Professor Associado, Instituto de Física, UFRGS, RS.

Guilherme Koszeniewski Rolim, First Line Service Physicist, Scienta Omicron, Germany.

Guilherme Sombrio, Research and Development Engineer, Smart Photonics, Netherlands.

Gustavo de M. Azevedo, Professor Adjunto, Departamento de Física, UFRGS, RS.

Henrique Trombini, Professor Adjunto, UFSPA, RS.

Horácio Coelho-Júnior, Postdoctoral, CBPF, RJ.

Igor Alencar, Professor Adjunto, Departamento de Física, UFSC, SC.

Irene Teresinha Santos Garcia, Professor Titular, Instituto de Química, UFRGS.

Ivan Rodrigo Kaufmann, SiC Process Development Engineer, Nexperia, Germany.

João Marcelo Lopes, Senior Scientist, Paul-Drude-Institut für Festkörperelektronik, Germany.

José Henrique Rodrigues dos Santos, Professor Adjunto, Departamento de Física, UFRGS.

Josiane Bueno Salazar, Supervisora de Proteção Radiológica, PhyMED Consultores em Física Média e Radioproteção Ltda, RS.

Leandro Langie Araujo, Professor Adjunto, Departamento de Física, UFRGS, RS.

Ludmar Guedes Matos, Process Quality Engineer, Instituto de Pesquisas Eldorado, SP.

Mariana de Mello Timm, Postdoctoral Researcher - University of Montpellier, France.

Mateus Dalponte, Head of Data Science, Axur Digital Risk Monitoring, RS.

Mauricio de Albuquerque Sortica, Researcher Engineer, Tandem Laboratory, Uppsala University, Sweden.

Milena Cervo Sulzbach, Design Engineer, ASML, Netherlands.

Rafael Peretti Pezzi, Design Engineer, ASML, Netherlands.

Rafaela Debastiani, Postdoctoral Research Scientist, Karlsruher Institut für Technologie, Germany.

Raquel Giulian, Professor Associado, Instituto de Física, UFRGS, RS.

Raquel Silva Thomaz, Professor Adjunto, Faculdade de Física, PUCRS, RS.

Raul Carlos Fadanelli Filho, Professor Adjunto, Departamento de Física, UFRGS, RS.

Roberto M. S. dos Reis, Scientific Officer, Northwestern University, Illinois, USA.

Rossano Lang Carvalho, Professor Adjunto, Instituto de Ciência e Tecnologia, UNIFESP, SP.

Samir de Morais Shubeita, Researcher Engineer, Dalton Cumbrian Facility - University of Manchester, England.

Shay Rebbot, Senior Research Engineer, CEA Leti, France.

Silma Alberton Corrêa, Professor Adjunto, Instituto de Química, UFRGS, RS.

Suzana Bottega Peripolli, Professora Adjunta, Departamento de Engenharia Mecânica, UERJ, RJ.

Taís Orestes Feijó, First Line Service Physicist, Scienta Omicron, Germany.

Tiago Silva de Ávila, Professor, Instituto Federal de Educação Ciência e Tecnologia Farroupilha, RS.

Vagner Zeizer Carvalho Paes, Data Scientist at Bright Photomedicine, PR.

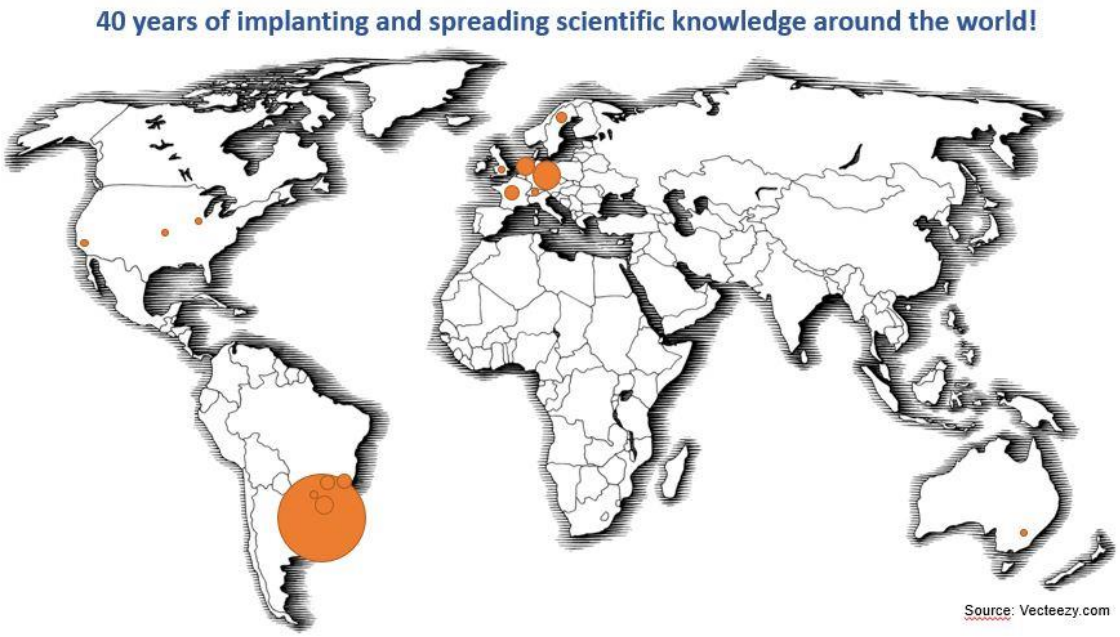

Brazilian Collaborators

Adriano Feil, Escola de Ciências, PUCRS. Roberto Hübler, Escola de Ciências, PUCRS.

Cecilia Veronica Nunez, Instituto Nacional de Pesquisas da Amazônia (INPA).

Henrique Trombini, Departamento de Ciências Exatas e Sociais Aplicadas, Universidade Federal de Ciências da Saúde Porto Alegre, RS.

Igor Alencar Vellame, Departamento de Física, Universidade Federal de Santa Catarina, UFSC, SC.

Jairo José Zocche, Laboratório de Ecologia de Paisagem e de Vertebrados, Universidade do Extremo Sul Catarinense, SC.

Juliana da Silva, Laboratório de Genética Toxicológica, Universidade Luterana do Brasil, RS.

June Ferraz Dias, Instituto Oceanográfico, Universidade de São Paulo, SP.

Neusa Fernandes Moura, Escola de Química e Alimentos, FURG, RS. Gerado Gerson Bezerra de Souza, Instituto de Química, UFRJ.

João Antônio Pêgas Henriques, Instituto de Biociências, Universidade Federal do Rio Grande do Sul, RS.

Sandro Guedes de Oliveira, Departamento de Raios Cósmicos e Cronologia, Universidade de Campinas, SP.

Vanessa Moraes de Andrade, Laboratório de Biologia Celular e Molecular, Universidade do Extremo Sul Catarinense, SC.

International Collaborators

Bernt Johannessen, Australian National Science and Technology Organization (AN-STO), Australian Synchrotron, Australia.

Björn Winkler, Institute of Geosciences, Goethe-Universitat Frankfurt am Main, Germany.

Bruno Canut, Institut des Nanotechnologies de Lyon, Université Lyon 1, Lyon, France.

Christina Trautmann, Department of Materials Research, GSI Helmholtzzentrum für Schwerionenforschung, Germany.

DaeWon Moon, DGIST TechnoJungAngDaeRo 333, Dalsung, Daegu, Korea.

Daniel Primetzhofer, Department of Physics and Astronomy / Ion Physics Uppsala University.

Gabriela Hoff, Universita di Cagliari Dipartimento di Fisica, Monserrato, Italy.

Jean-Jacques Pireaux, Namur University, Namur, Belgium.

João Marcelo J. Lopes, Paul-Drude-Institut für Festkörperelektronik (PDI), Berlin, Germany.

Katarina Vogel-Mikus, Department of Biology, Biotechnical Faculty, University of Ljubljana, Ljubljana, Slovenia.

Leonard C. Feldman, Department of Physics and Astronomy, Rutgers - The State University of New Jersey, Piscataway, NJ, U.S.A.

Limin Zhang, School of Nuclear Science and Technology, Lanzhou University, Lan-zhou, P. R. China.

Maarten Vos, Australian National University, Canberra, Australia. Gregor Schiwietz, Helmholtz-Zentrum Berlin (HZB), Berlin, Germany.

Mahesh Kumar, Indian Institute of Technology Jodhpur, India.

Mário Simeón Pomares Alfonso, Instituto de Ciencia y Tecnología de Materiales, Uni-versidad de la Habana.

Melissa K. Santala, School of Mechanical, Industrial, and Manufacturing Engineering, Oregon State University, USA.

Patrick Kluth, Department of Electronic Materials Engineering, Australian National University, Australia.

Saul Larramendi Valdes, Departamento de Física Aplicada, Facultad de Física, Universidad de la Habana.

Stella Ramos-Canut, Institut Lumière Matière, Université Lyon 1, Lyon, France.

Facilities

The Ion Implantation Laboratory has three accelerators that provide a wide variety of positive ions in a broad energy range, they are:

- 3 MV Tandetron accelerator;
- 500 kV and 250 kV accelerators.

3 MV Tandetron

500 kV accelerator

250 kV accelerator

Besides the accelerators, the laboratory has the following additional facilities:

- Photoluminescence laboratory;
- Clean-room;
- Furnaces, ovens and reactor chambers;
- Workshop.

Furnaces and reactors

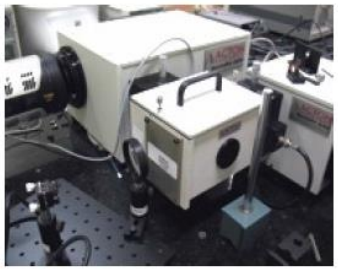

Optical characterization

Clean-room

User's Highlights
Selected among their published articles

Elemental characterization of sparkling wine and cork stoppers

Carla Eliete Iochims dos Santos

The variations of the elemental concentrations in sparkling white wine and respective cork stoppers throughout 18 months of storage time were determined with the PIXE (Particle-Induced X-ray Emission) technique. Three portions of the cork stoppers were analyzed: the top part (external layer), the inner part (bulk layer) and the bottom layer (which was in contact with the sparkling wine). Elements such as Na, Mg, Si, P, S, Cl, K, Ca, Mn, Fe, Zn and Rb were determined for both cork stoppers and sparkling wine samples. Similar concentrations of Si, P, S,

Cl and Ca were found in the external and bottom layers of the corks. Distinct behaviors of the changes in the elemental concentrations as a function of the time were observed for cork stoppers and sparkling wines. The concentrations of Mg, S, K, Ca, Cu, Sr and Ba increased in the bottom layer of the cork as a function of storage time. On the other hand, concentrations of Al, Si, Cl, Ti, Zn and Br proved to be invariant, while the concentrations of P and Fe showed a slight decrease. Concerning the sparkling wine, an increasing trend of elemental concentrations was observed for most elements throughout the storage time.

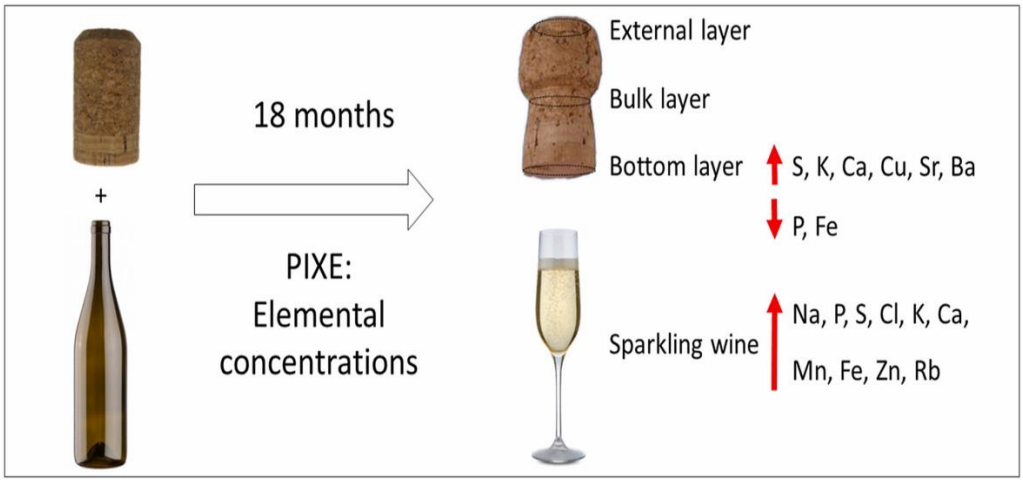

Elemental composition of sparkling wine and three different parts of the cork stopper throughout the storage time. An increasing concentration was observed in the wine for the most part of the detected elements.

Paper reference:

Elemental characterization of sparkling wine and cork stoppers, R. Debastiani, C. E. I dos Santos, and J. F. Dias, Current Research in Food Science, 4 (2021) 670-678.

Nitrogen Incorporation into Ta Thin Films Deposited over Ti6Al4V: A Detailed Material and Surface Characterization

Cesar Aguzzoli

Ti6Al4V is widely used as a metallic biomaterial and in cutting-edge fields of biomedicine that must comply with emerging technological demands such as smart wearable pieces and implantable electronic devices. In this work, we perform a duplex process where pure tantalum thin films were deposited over Ti6Al4V substrate by magnetron sputtering followed by a post-treatment consisting of plasma nitriding. Plasma nitrided Ta films exhibit improvement in wettability and increased roughness, both of which are attributed to the texturing of the surfaces. The RBS results plus SIMRA simulations allow to analyze the thin film stoichiometry and thickness variation according to the processes carried out. XRD spectra provided information of the nitrogen incorporation in tantalum, as a Ta containing phase was observed in plasma nitrided films. In summary, nitrogen-enriched tantalum films tailored by duplex process of sputtering/plasma nitriding fulfills important characteristics of quality coatings, synergistically.

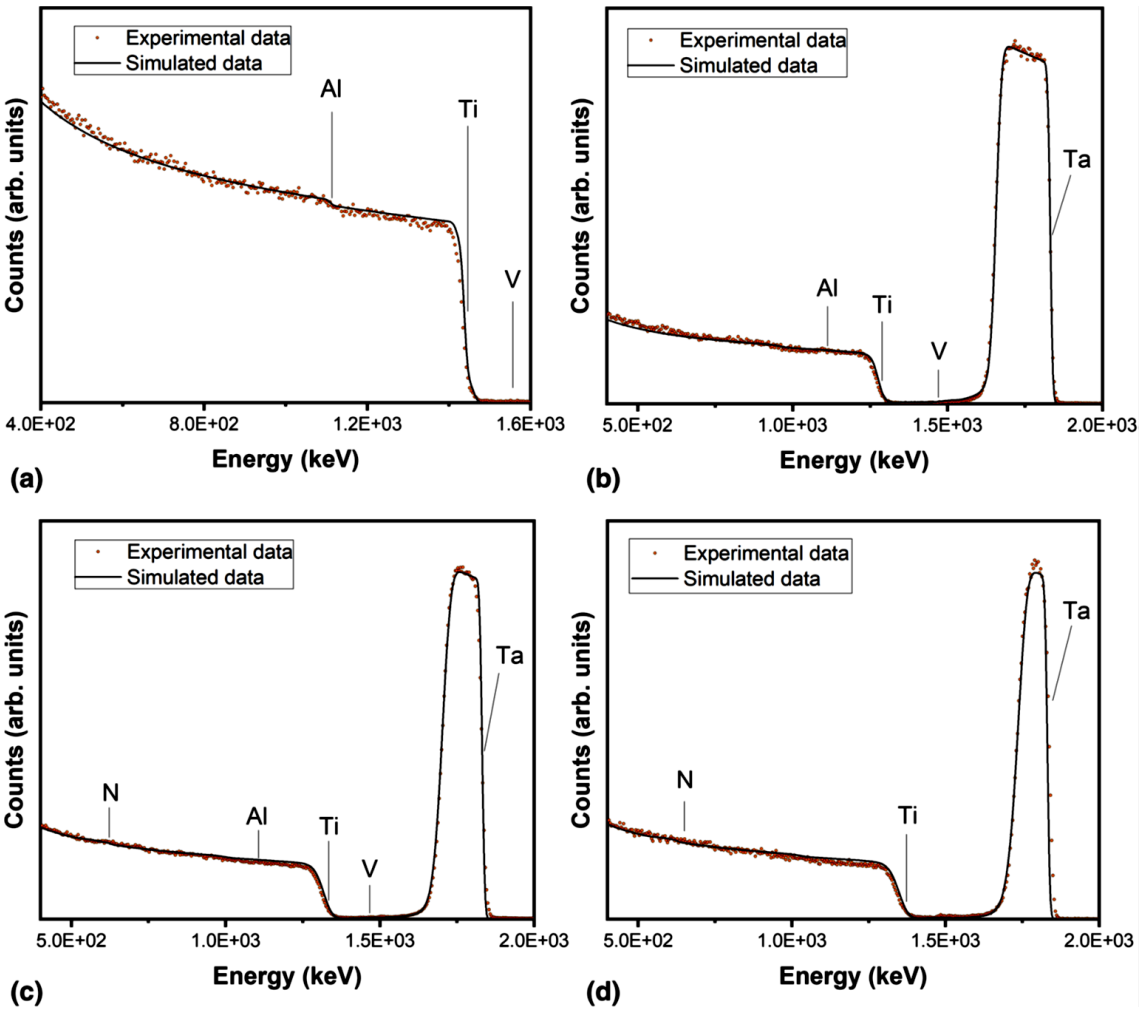

RBS spectrum for the Ti6Al4V substrate (a), Ti6Al4V-Ta (b), Ta(N10)-Ti6Al4V (c), and Ta(N30)-Ti6Al4V (d)

Paper reference:

Nitrogen Incorporation into Ta Thin Films Deposited over Ti6Al4V: A Detailed Material and Surface Characterization, C. P. Fontoura, A. E. D. Maddalozzo, M. M. Rodrigues, R. A. Barbieri, J. da S. Crespo, C. A. Figueroa, and C. Aguzzoli, Journal of Materials Engineering and Performance, 30 (2021) 4094–4102.

WS_2 obtained by sulfurization of deposited WO_3 films

Cláudio Radtke

Transition metal dichalcogenides (TMDs) have emerged as a class of 2D materials presenting properties to be explored in many technological fields. The most remarkable one is probably the possibility to tune the bandgap of these materials by modifying the number of layers composing the stack. Moreover, there is a transition from an indirect to direct bandgap when one reaches a monolayer. In order to fully explore such properties, obtaining lateral homogeneous stacks with the desired number of layers is mandatory. Several techniques have been proposed with this goal. Most of them are based in a chemical vapor deposition (CVD) process in which Sulfur (S) and a metal oxide are simultaneously evaporated and carried by a gas to a substrate surface where the TMD is formed. This approach has intrinsic difficulties like inhomogeneous precursors supply and, in the specific case of tungsten sulfide (WS_2), the high thermal budget for tungsten oxide (WO_3) evaporation.

Sulfurization of WO_3 films can be an alternative to conventional chemical vapor deposition processes were both WO_3 and S must be transported in the gas phase. Nevertheless, W loss and incomplete sulfurization were reported using this approach, constituting experimental hurdles to obtain WS_2 layers with a specific thickness. The moment of S introduction in the process showed to play a decisive role, determining the obtention of a completely

sulfurized layer or a modified oxide. Results evidenced that during a certain period, while sulfurization conditions are not efficient (S heating zone below 170 °C), WO_3 annealing induces morphological and structural modifications (mainly crystallization) which modify oxide's reactivity towards S. With this knowledge, efficient sulfurization strategies can be designed aiming at obtaining WS_2 layers with the desired characteristics.

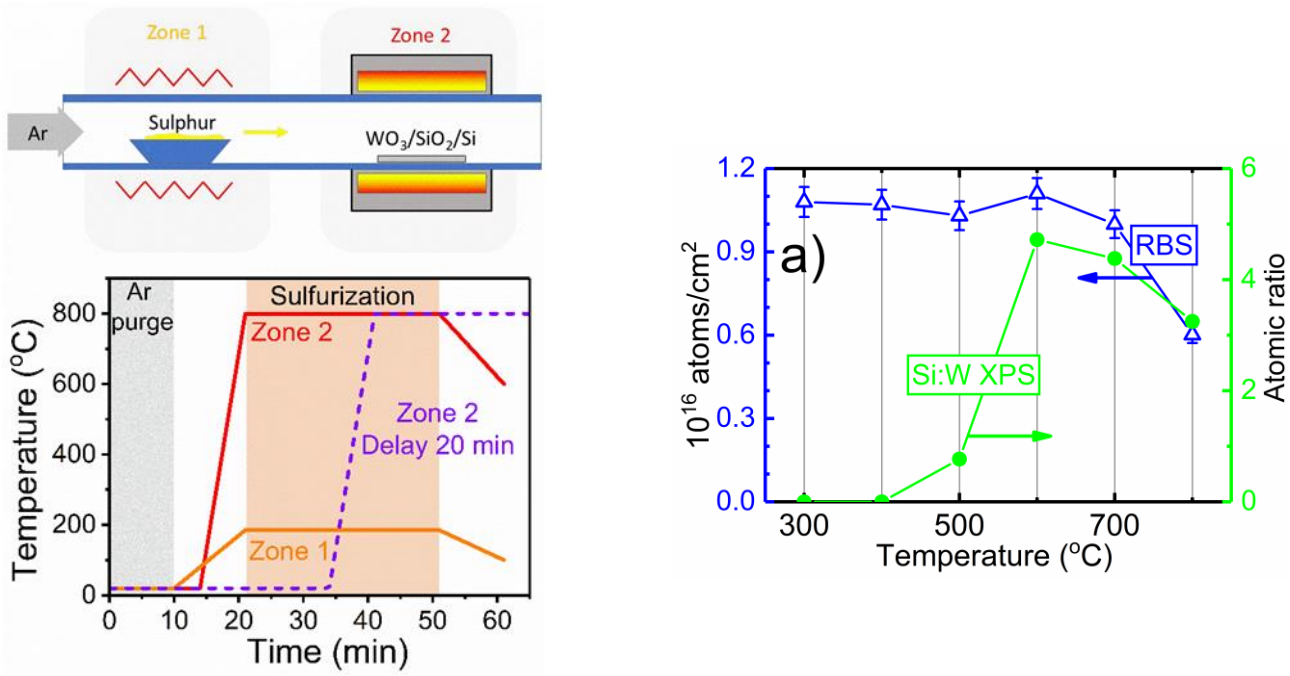

(Left side) Temperature profiles of the two heating zones of the sulfurization system. Above the graph, there is a sketch identifying the heating zones. The violet dashed line stands for a process with a 20 min delay with respect to the original setup (red line). (Right side) Stability of WO3 films at different annealing temperatures. W areal densities (open blue symbols) obtained by RBS of WO3/Si samples submitted to annealing at the indicated temperatures. Respective Si:W atomic ratios (solid green symbols) determined by XPS are also shown.

Paper reference:

Timing of sulfur introduction in the sulfurization of WO_3 films dictates WS_2 formation, D.S. Cabeda, G.K. Rolim, G.V. Soares, A.M.H. de Andrade, and C. Radtke, Applied Surface Science, 610 (2023) 155488.

Thermal behaviour of Cu and Au nanoparticles grown on CeO_2 thin films

Henrique Trombini

Ceria, known for its ability to enhance metal dispersion and greater resistance to thermal sintering, is a useful oxide support for various metal catalysts. In particular, Cu/Au nanoparticles supported on CeO_2 have been used for numerous applications in catalysis and electroreduction. However, the thermal behaviour of Cu/Au/CeO_2 model catalysts is not well understood. In this article, the temperature dependence of the composition profile of Cu/Au particles on CeO_2 thin films grown on Si(111) was characterized using medium energy ion scattering (MEIS), atomic force microscopy (AFM), and X-ray photoelectron spectroscopy (XPS). XPS analysis reveals that the ceria film is initially almost pure CeO_2 in composition, and deposition of Au onto the CeO_2/Si(111) surface leads to a slightly lower Ce(IV):Ce(III) ratio. Further deposition of Cu onto the recovered Au/CeO_2/Si(111) surface leads to a reduction of Ce(IV). These observations indicate the formation of pure Au and pure Cu particles with some Cu deposition onto Au particles. The most physically realistic model for the sample after annealing to 525 K involves the formation of hemispherical alloyed CuAu particles, which are relatively

thermally stable up to at least 450 K. When a sample prepared by deposition of Cu followed by Au onto CeO_2/Si(111) is exposed to air, XPS reveals the presence of Cu(II) species, which are reduced to Cu/Cu(I) with increasing annealing temperature. Annealing to 375 K caused desorption of weakly bound adsorbates, and MEIS revealed that under these conditions, the sample consisted of nanoparticles with an Au-rich core and a Cu-rich shell. Annealing to higher temperatures resulted in the formation of alloyed particles. Overall, this study provides insights into the composition and thermal stability of Cu/Au/CeO_2 model catalysts and their potential use in selective hydrogenation reactions.

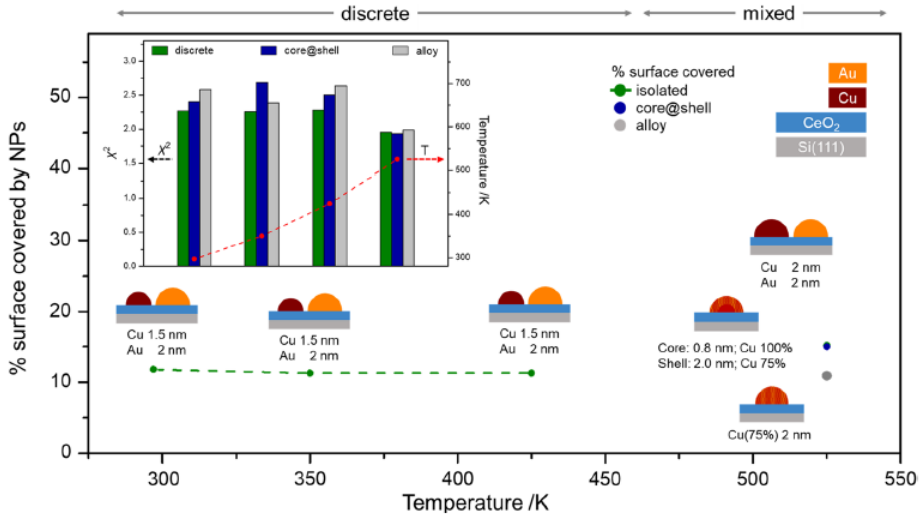

Nanoparticle radii, morphology and % of surface covered by nanoparticles as a function of annealing temperature for the samples prepared by the deposition of 0.14 ML Au followed by 0.6 ML Cu onto a ~2 nm CeO_2 film on Si(111) as deposited (~300 K) and annealed to 350, 425 and 525 K. In the inset, Chi-square analysis for the same samples obtained from the three ion backscattering angles.

Paper reference:

Thermal behaviour of Cu and Au nanoparticles grown on CeO_2 thin films, R. Megginson, F. Grillo, S. M. Francis, V. Z. C. Paes, H. Trombini, P. L. Grande, A. K. Rossall, J. A. van den Berg and C. J. Baddeley, Applied Surface Science, 575 (2022) 151656.

The influence of radiation damage on electrons and ion scattering measurements from PVC films

Henrique Trombini

A new method for evaluating changes in sample composition caused by radiation fluence is presented in this research paper. The paper explores the use of electron Rutherford backscattering (ERBS) and reflection energy loss spectroscopy (REELS) to investigate the effect of irradiation fluence on PVC, a commonly used polymer. ERBS was used to measure the energy transfer in large-angle elastic scattering of keV electrons from nuclei. The results of the study are compared to earlier polymer ERBS results to explore the possibility of describing deviations of the observed intensities in terms of radiation damage. While x-ray yield-based methods can measure the change in intensity of a component very well, the present method was better suited to assessing whether the initially measured intensity corresponded to the nominal stoichiometry. The measurements showed similar Cl depletion profiles and good agreement was found with Cl depletion based on Cl LMM

Auger electrons, which is an order of magnitude more surface sensitive. Electron scattering at high energies can provide insight into several aspects of radiation damage, and the results can be interpreted consistently with those obtained from ion-scattering experiments. Overall, the study provides a valuable contribution to the field of radiation damage in materials, demonstrating a new method of assessing sample composition changes as a function of radiation fluence using ERBS and REELS. The method was successful in measuring changes in PVC caused by irradiation fluence, and the results were found to be consistent with those obtained from ion-scattering experiments like Rutherford Backscattering Spectroscopy (RBS) and Medium Energy Ion Scattering (MEIS). This research paper has important implications for those studying the effects of radiation on materials and provides a valuable tool for assessing sample composition changes.

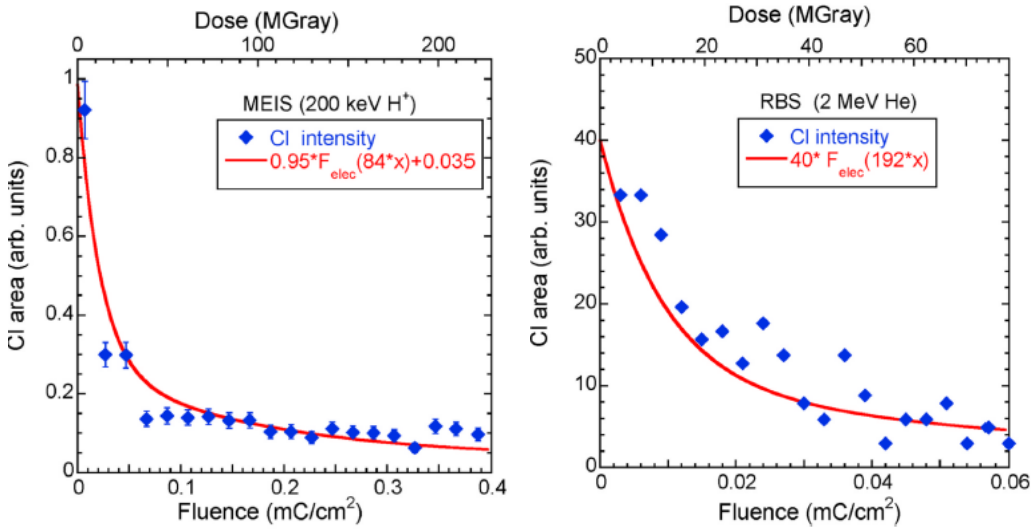

The Cl intensity as measured by MEIS (left) and RBS (right) together with the decay curve as determined by ERBS (using $\frac{N_{Cl}(x)}{N_{Cl}(0)} = (1-A)e^{-k_1 x} + Ae^{-k_2 x}$*) but scaled for the horizontal axis according to the ratio of electronic stopping of e- and the ion used. For MEIS a small quantity (0.035) was added corresponding to the dark count rate of the detector.*

Paper reference:

The influence of radiation damage on electrons and ion scattering measurements from PVC films, B. P. E. Tee, M. Vos, H. Trombini, F. F. Selau, P. L. Grande, R and Thomaz, 179 (2021) 109173.

Nanoparticle emission by electronic sputtering of ionic single crystals

Igor Alencar

Swift heavy ions impinging on solids are able to eject a very large number of particles in a phenomenon denoted electronic sputtering, which is a consequence of the predominant energy deposition by electronic excitation. An astonishing amount of mass could be sputtered in a single ion impact, comprising intact and fragmented molecules, clusters of atoms or atomized species. Albeit several basic aspects of electronic sputtering have already been clarified, many mechanistic aspects are not yet well understood. An example is the strong jet-like component of emission (i.e. preferred emission at the surface normal) observed for ionic crystals. Applying complementary state-of-the-art characterization techniques, namely Transmission Electron Microscopy (TEM), Atomic Force Microscopy (AFM) and Medium Energy Ion Scattering (MEIS), to investigate the surface of silicon wafers and copper grids used as ejecta catchers during the irradiation of calcium fluoride single

crystals with 180 MeV Au primary ions at three different angles of incidence, we report the emission of crystalline nanoparticles from bulk materials. This comprehensive characterization allowed us to establish the spherical nature of the nanoparticles and correlate their emission to the jet-like component. Additionally, processes involving only defect diffusion, Knudsen layer, thermal spike, Coulomb explosion or single exciton cannot account for the observed results and, therefore, do not describe properly the underlying physics for the electronic sputtering scenario. Additionally, confining the effective depth for energy deposition closer to the target surface may enhance the particle contribution to electronic sputtering. Such conclusions might be directly extrapolated to other ionic crystals and, perhaps, to dielectric materials in general. Moreover, these new insights about electronic sputtering shed light, for instance, into beam optimization for mass spectrometry with high energy primary ions.

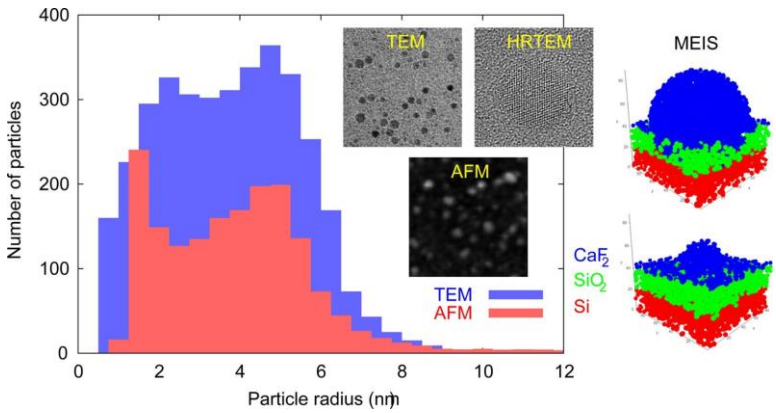

Radii distribution of nanoparticles as determined by AFM and TEM. Insets show typical particle images and the best fitting model obtained for MEIS.

Paper reference:

Nanoparticle emission by electronic sputtering of CaF_2 single crystals, I. Alencar, M. Hatori, G. G. Marmitt, H. Trombini, P. L. Grande, J. F. Dias, R. M. Papaléo, A. Mücklich, W. Assmann, M. Toulemonde, C. Trautmann, Applied Surface Science, 537 (2021) 147821.

Radiation effects in diamond by 14 MeV Au ions

Igor Alencar

Diamond is the hardest natural material. Its properties, such as high thermal conductivity, high resistivity, high breakdown electric field and wide bandgap, are exploited in numerous applications. A high atomic displacement energy due to the strong covalent bonding as well as the low atomic number of carbon results in a radiation hard material. For safe, reliable use as a radiation detector, it is mandatory to understand the damage induced by radiation. Combining several techniques, namely Atomic Force Microscopy (AFM), Raman spectroscopy, X-Ray Reflectivity (XRR), Electron Backscatter Diffraction (ESBD) and Rutherford Backscattering Spectrometry (RBS), we presented a near surface evaluation of the radiation damage induced by 14 MeV Au ions in diamonds. The samples consists of high-pressure, high-temperature synthesized single crystals, chemical vapor deposition grown single crystals and polycrystalline pellets. The swelling observed by AFM

indicates that the irradiation reached a critical density, where the induced alterations are irreversible. Raman spectroscopy illustrates the partial graphitization of the lattice, as a consequence of the breaking of sp3-bonds and formation of sp2-bonds. XRR analysis indicate the formation of subsurface layers with reduced density, with an amorphization of the first 5-20 nm. Such an observation is further supported by the significant decrease in the quality of the EBSD patterns. Finally, RBS provides the means to unravel the Au implantation spatial distribution. For this purpose, 3.0 to 4.0 MeV He ions were used. At such energies, the non-Rutherford, resonant scattering 12C(α,α)12C plays a crucial role and it must be taken into account for a proper spectra evaluation. When compared to simulated spectra, some experimental results are puzzling. Such discrepancies raise the question whether the available non-Rutherford cross sections are suitable at our experimental conditions.

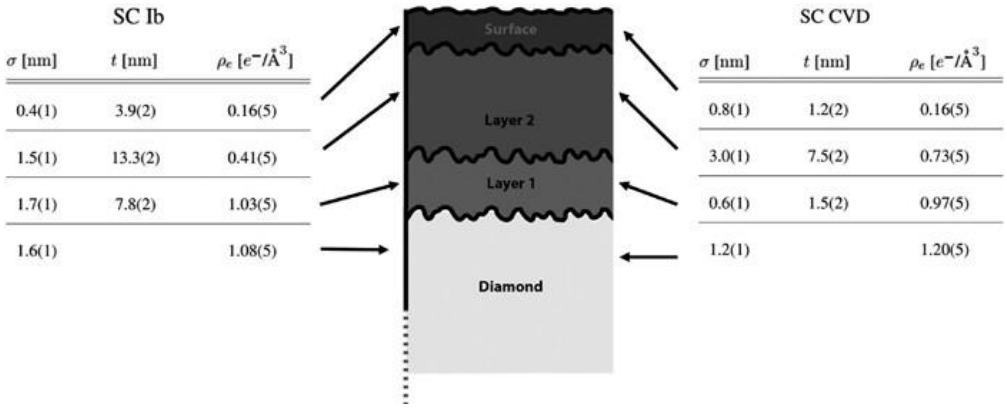

Best fitting model for XRR data from two different single crystals showing roughness, thickness and density of the subsurface layers. These results are corroborated by Raman spectroscopy and EBSD patterns.

Paper reference:

Surface and subsurface damage in 14 MeV Au ion-irradiated diamond, K. Bunk, I. Alencar, W. Morgenroth, F. Bertram, C. Schmidt, D. Zimmer, P. Gruszka, M. Hanefeld, L. Bayarjargal, C. Trautmann, B. Winkler, Journal of Applied Physics, 130 (2021) 105303.

The Potentialities of Accelerator-Based Techniques as an Analytical Tool for Forensics

Johnny Ferraz Dias

We discuss how different accelerator-based techniques can be employed synergistically as a powerful analytical tool for forensic studies of foodstuff. Brazilian and Jamaican coffees were chosen as a showcase due to its popularity and potential risk of adulteration and/or falsification. Comprehensive characterization of major and trace elements, age since production and compound contents were achieved using different techniques, including PIXE (Particle-Induced X-ray Emission), FTIR (Fourier Transform Infrared), and AMS-14C (Accelerator Mass Spectrometry – Radiocarbon Analysis). While PIXE provides information on the elements present in the samples, FTIR probes the types of compounds through their vibrational

spectra. Finally, AMS-14C is capable of dating organic samples regarding their harvesting time. Five different laboratories from research institutions around the world took part in the experiments.

The integration of the results obtained with different techniques provided multifaceted perspectives on the coffee under study, thus allowing a direct assessment of the material for forensic purposes such as authentication, determination of provenance, and combat counterfeiting.

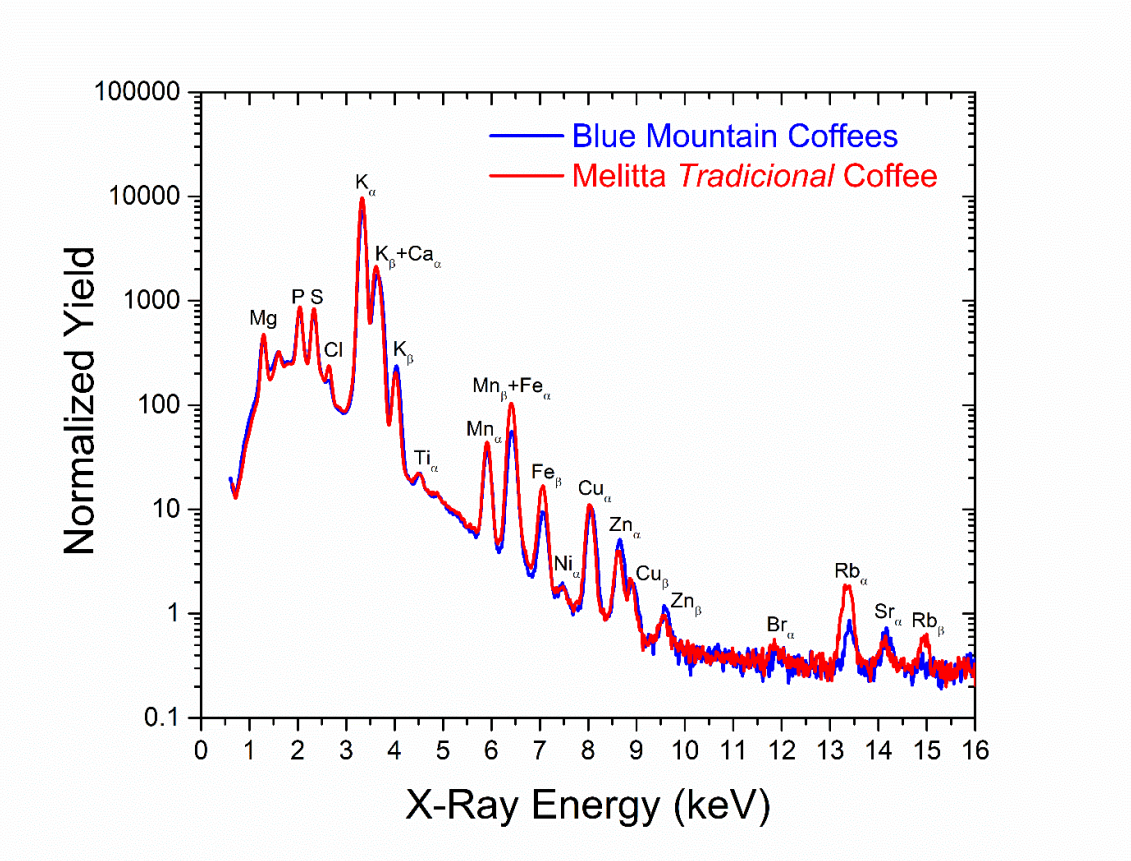

X-ray yield as a function of the X-ray energy. The yields of all measurements were normalized by the charge accumulated during the experiments. Each spectrum represents an average over all measurements carried out for the Melitta Tradicional (red line) and for Blue Mountain (blue line) coffees. The elements are identified by the respective atomic transitions (alpha or beta).

Paper reference:

The potential of accelerator-based techniques as an analytical tool for forensics: The case of coffee, P. Chytry, G. M. S. Souza, R. Debastiani, C. E. I. dos Santos, J. M. R. Antoine, A. Banas, K. Banas, L. Calcagnile, M. Chiari, I. Hajdas, M. Molnar, P. Pelicon, N. Pessoa Barradas, G. Quarta, F.S. Romolo, A. Simon, J.F. Dias, Forensic Science International, 335 (2022) 111281/1-111281/10.

Bohr's stopping-power formula derived for a classical free-electron gas

Pedro Luis Grande

Bohr's centenary stopping-power formula is rederived for a free electron gas (FEG) system within the framework of nonrelativistic classical mechanics. A simple and more concise expression for the stopping power of charged particles in FEG is demonstrated on classical grounds. Using semiclassical arguments and the Euler-Maclaurin well-known mathematical formula, Bloch's correction that links Bethe's quantum theory to Bohr's classical model is also recovered. The proposed semiclassical stopping-power formula contains the main physical ingredients for a general stopping formula applicable to different systems and energies and facilitates computational calculations. We first considered the slowing down of a point charge (Z1) in a classical FEG with density n where the electrons are at rest (static FEG). In the reference frame where the projectile is at rest, there is a beam of

electrons of density n and velocity v that is scattered by the fixed-point charge or ion (see Fig. 1). We derived a formula for the stopping power (see ref. [1]) of charged particles in a classical system of electrons at rest with initial-state density n (classical static FEG), assuming a central potential for the ion-electron interaction. It gives the same results as Bohr's classical theory in its range of validity. This stopping formula captures the basic stopping processes regarding target ionization and excitation and can be applied to real systems after considering different target densities, shell corrections, screening, and charge states of the projectile.

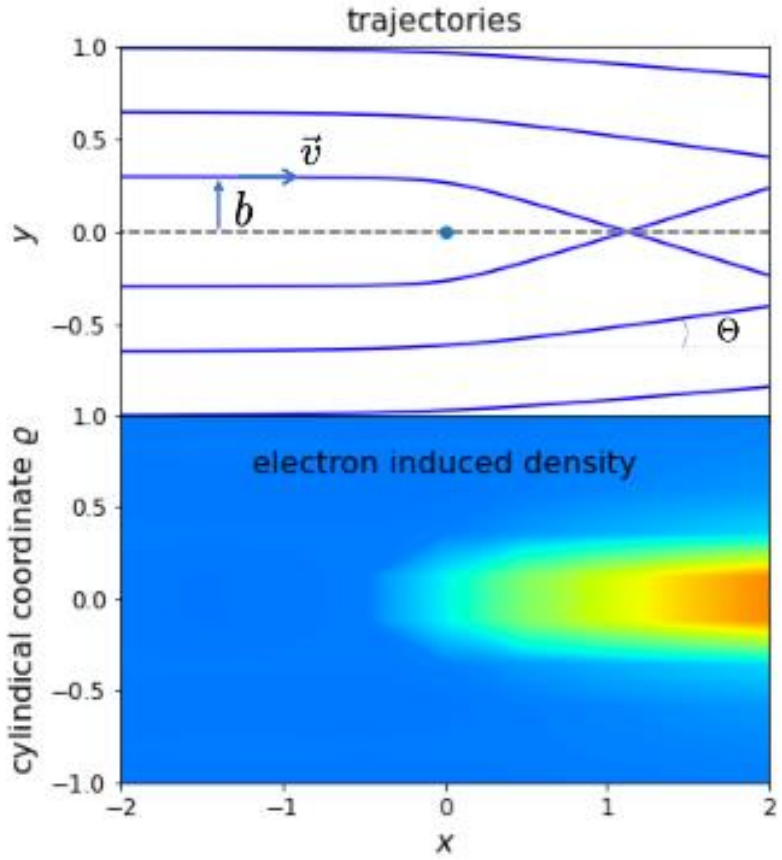

Illustration of the electron trajectories (top) and induced density (below) for an ion at (x = 0, y = 0, z = 0). Electrons come from left to right with velocity v and impact parameter b. x is the direction of the motion, and q the scattering angle. Simulations were performed for a

proton in the laboratory system with v = 5 and electron Wigner-Seitz radius rs = 2.07 in atomic units.

Paper reference:

Bohr's stopping-power formula derived for a classical free-electron gas, P. L. Grande, Physical Review, A (2021) 012807-1.

Model dielectric functions for ion stopping

Maarten Vos and Pedro Luis Grande

The interaction of fast, charged particles with the matter has been a central topic of research for a long time. Bohr used it to test his emerging understanding of the quantum nature of matte. Bethe derived a first description, fully consistent with modern quantum physics, and further refinements were due to Lindhard, to name only the major players. Besides its fundamental interest, the topic is studied for its importance in technological fields like ion beam analysis and ion beam modification of materials. More recently, it has attracted attention within the context of ion-beam-based cancer therapy. We describe a set of energy (ω) and momentum (q)-dependent dielectric functions with the same shape of the loss function (see Fig. 1) in the optical limit (q = 0) and thus the same mean ionization energy I

but different behavior away from q = 0. The corresponding proton-stopping values differ especially at lower energies. Within the Bethe formula, the stopping only depends on the mean excitation energy I. These models display thus different shell corrections, defined as the deviation from the stopping from the Bethe values. Shell-correction contributions originate equally from collisions with low momentum transfer and with high momentum transfer. Intermediate q collisions do not contribute to the shell corrections. At high q the shell corrections are related to the width of the loss function at these q values (which is proportional to the momentum distribution of the electrons [“Compton profiles”]) or, for classical models, from a shift in position. The low-q contribution is related to the plasmon dispersion. For further details please see Ref. [1].

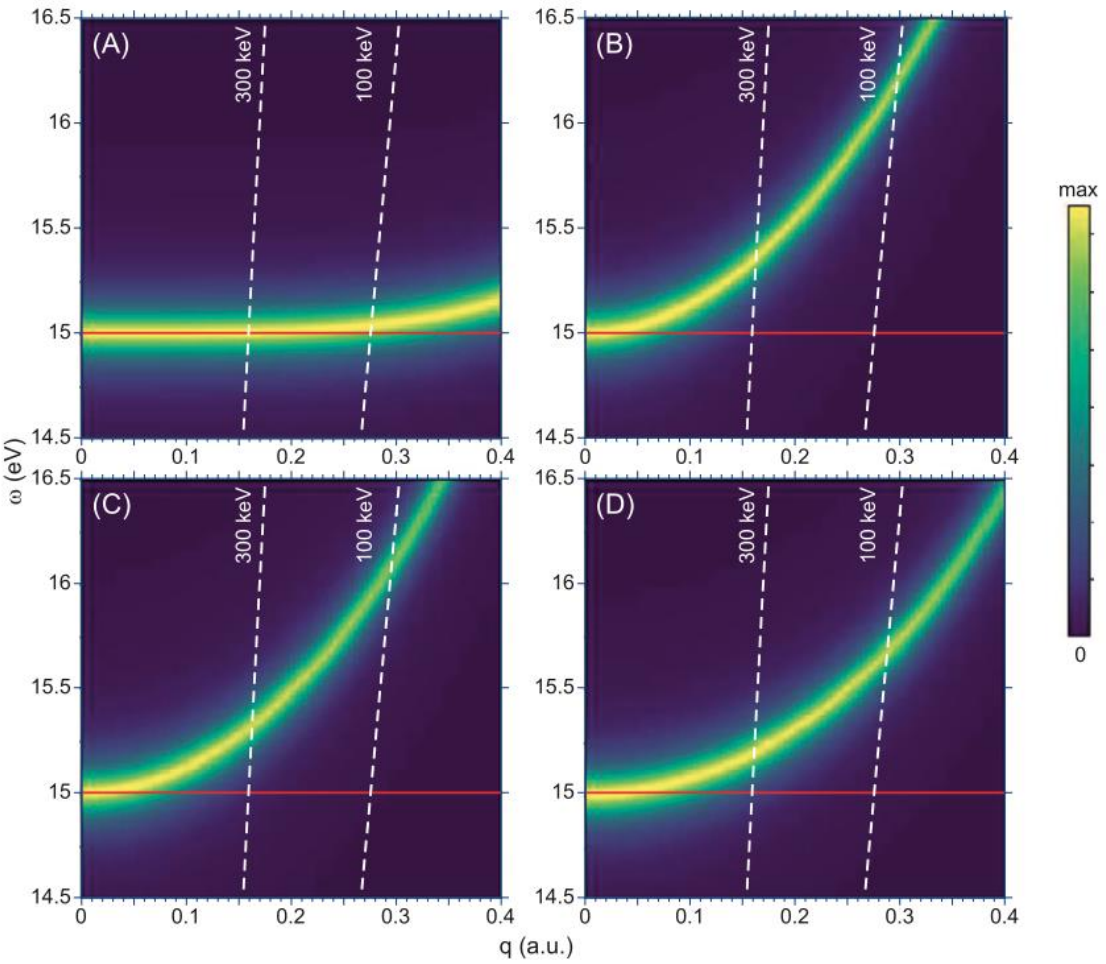

The ELF distribution of the extended Drude(A), Drude Lindhard(B),Mermin(C), and Mermin–Levine–Louie (D) dielectric function for small momentum values and energies close to the plasmon energy. The red line is again the dispersion of our "ad hoc" dielectric function. The dashed lines are the qv lines at 100 keV and 300 keV.

Paper reference:

Model dielectric functions for ion stopping: The relation between their shell corrections, plasmon dispersion and Compton profiles, M. Vos and P. L. Grande, Advances in Quantum Chemistry, ISSN 0065-3276 (2022) 267-301.

$In_{1-x}Ga_xSb$ nanofoams made by ion irradiation of sputtered films: Atomic composition and structure

Raquel Giulian

This article reports on the atomic composition and structural changes induced by ion irradiation in $In_{1-x}Ga_xSb$ films deposited by magnetron sputtering on SiO_2/Si. Samples with x values equal 0, 0.2, 0.4, 0.5 and 1 were irradiated with 16 MeV Au^{+7} ions, in the fluence range 5×10^{13} – 2×10^{14} cm^{-2} (3×10^{14} for GaSb) and the structure and atomic composition of the films were investigated. Upon irradiation, all films attain a nanofoam-like structure, and the most pronounced swelling was observed in ternary films with 20% Ga atomic concentration. With particle induced x-ray emission technique, we identified the presence of C, O, Ga, In and Sb, with C and O concentrations significantly higher in the nanofoams, compared to the as-deposited films. Rutherford backscattering spectrometry analysis showed the atomic composition of the ternaries is not uniform, but forms two layers with slightly different relative atomic concentrations, specially after irradiation, with C and O uptake greatly enhanced by ion irradiation, more pronounced towards the surface. Grazing incidence x-ray diffraction analysis revealed that ion irradiation with total fluence of 2×10^{14} cm^{-2} induces amorphization of the ternaries, except for samples with 50% Ga, which remain polycrystalline, despite the ion-induced porosity.

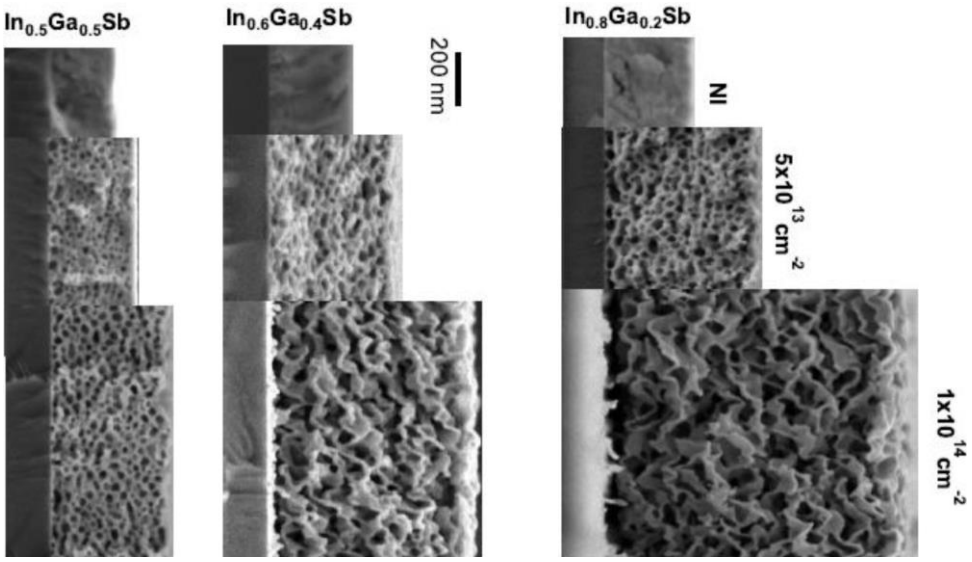

Scanning electron microscopy micrographs of In1-xGaxSb films, as-deposited and irradiated with 16 MeV Au+7 ions at different fluences. NI – not irradiated.

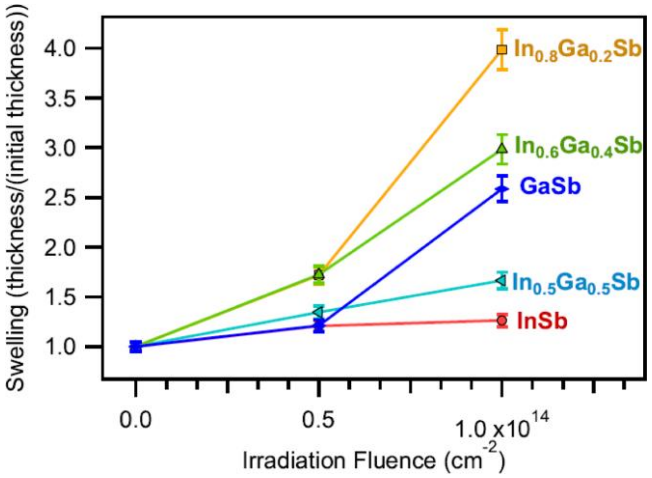

Swelling as a function of irradiation fluence for $In_{1-x}Ga_xSb$ films irradiated with 16 MeV Au^{+7} ions. Film thicknesses were measured directly from scanning electron microscopy micrographs.

Paper reference:

$In_{1-x}Ga_xSb$ nanofoams made by ion irradiation of sputtered films: Atomic composition and structure, R. Giulian, C. A. Bolzan, L. T. Rossetto, A. M. H. de Andrade and J. F. Dias, Thin Solild Films, 753 (2022) 139263.

Local and extended atomic structure of strained polycrystalline $In_{(1-x)}Al_{(x)}Sb$

Raquel Giulian

$In_{(1-x)}Al_{(x)}Sb$ films were deposited on amorphous SiO_2 by magnetron sputtering with four different In/Al concentration ratios and the local and extended atomic structure were investigated through extended x-ray absorption fine structure (EXAFS) spectroscopy and grazing incidence x-ray diffraction (GIXRD) analyses, respectively. GIXRD showed the deposited films are strained polycrystalline, however, preserving the cubic symmetry of zincblende structure due to homogeneous compression. EXAFS analysis of In and Sb atoms in strained $In_{(1-x)}Al_{(x)}Sb$ films provided information about the inter-atomic distance distributions of the first three nearest-neighbor (NN) shells. For the first NN, the average cation-anion distances presented only the alloying effect, resembling the unstrained ternary alloy with a relaxation parameter of $\varepsilon = 0.77 \pm 0.01$ and $\varepsilon = 0.79 \pm 0.01$ for the dilute limit InSb:Al and AlSb:In, respectively, and with the extra structural modifications due to the strain factor appearing in higher coordination shells only. In the second NN shell distance it was observed that the strain effect is more pronounced in In-Al than In-In inter-atomic distance, which is, within uncertainty, independent of strain, evidencing an anisotropy in the process of accommodating the strain in the mixed sublattice, which is favored by bond bending over bond stretching, similarly to unstrained III-V ternary alloys. On the other hand, anion-anion distances exhibited a bimodal distribution,

showing a tendency to retain the values of unstrained pure compounds. The third NN shell mean distances vary linearly with concentration. Moreover, the core effect in $In_{(1-x)}Al_{(x)}Sb$ alloys was described via EXAFS demonstrating that elastic continuous medium theory is not adequate to describe this system. Using x-ray absorption near edge structure, it was observed that In K-edge position is constant with In/Al ratio in $In_{(1-x)}Al_{(x)}Sb$ alloys, whereas Sb K-edge position changed, evidencing its relation with the local atomic arrangement.

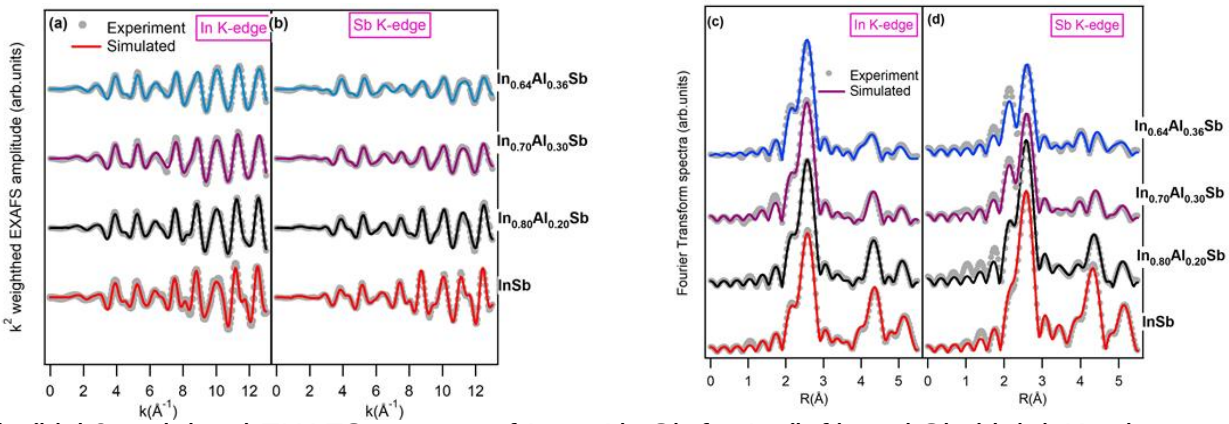

(a), (b) k2-weighted EXAFS spectra of $In_{(1-x)}Al_{(x)}Sb$ for In (left) and Sb (right) K-edges as a function of the photoelectron wavenumber. The corresponding Fourier transform spectra of $In_{(1-x)}Al_{(x)}Sb$ Sb for four different In/Al ratio concentrations at: (c)In K-edge and (d) Sb K-edge.

Paper reference:

Local and extended atomic structure of strained polycristalline $In_{1-x}Al_xSb$ alloys, C. A. Bolzan, B. Johannessen, Z. Wu and R. Giulian, Journal of Physics and Chemistry of Solids, 150 (2021) 109844.

Ion tracks in ultrathin polymer films: The role of the substrate

Raquel Thomaz

Ion tracks produced by swift heavy-ions were recorded in PMMA thin films of various thicknesses spun onto substrates of Si, SiO_2, and Au. We show that in films thinner than 40 nm craters induced by individual ions are modulated by the underlying substrate to a degree that depends on the transport properties of the medium, being larger in films deposited on SiO_2 as compared to the conducting Au layer. This is consistent with an inefficient coupling of the electronic excitation energy to the atomic cores in metals. On the other hand, the damage on films deposited on SiO_2 is not very different from the Si substrate with a native oxide layer, suggesting, in addition, poor energy transmission across the film/substrate interface. The experimental observations are also compared to calculations from an analytical model based on energy addition and transport from the excited ion track, which describe only partially the results.

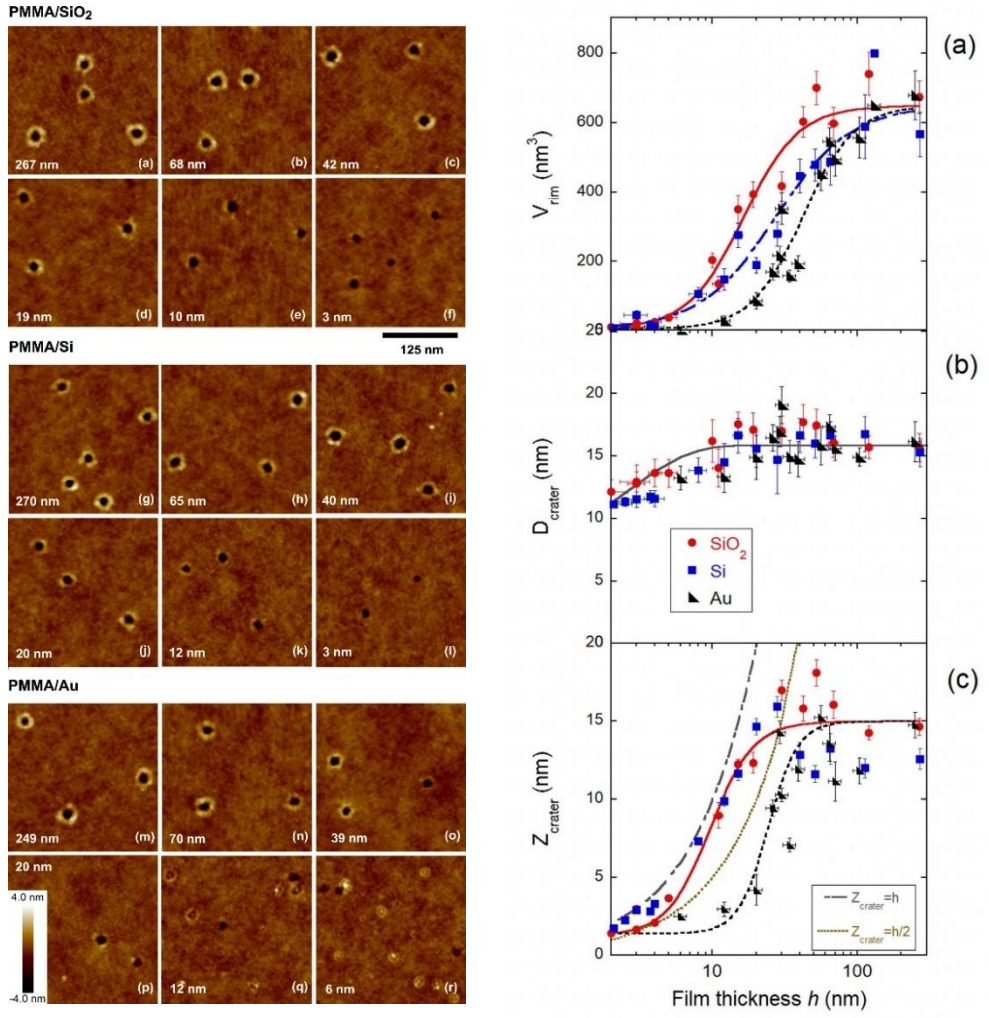

Left: AFM images of PMMA thin films of different thicknesses deposited on silicon dioxide (a-f), silicon (g-l), and Au (m-r) bombarded by 1.1GeV Au ions at normal incidence. The thickness of the films is given in each image. Very thin films on Au present also intrinsic defects, as seen in images, which are distinctively different from those produced by the ion impacts (q-r). Right: Averaged rim and crater dimensions produced by 1.1 GeV Au ions in PMMA films of various thicknesses h deposited on Si, SiO2 and Au substrates: (a) rim volume, (b) crater diameter, and (c) crater depth. The lines are guides to the eyes.

Paper reference:

Ion tracks in ultrathin polymer films: The role of the substrate, R. Thomaz, N. W. Lima, D. Teixeira, L. I. Gutierres, I. Alencar, C. Trautmann, P. L. Grande and R. M. Papaléo, Current Applied Physics, (2021) 91-97.

On the energy-loss straggling of protons in elemental solids: The importance of electron bunching

Raul Carlos Fadanelli

In this work we investigate the energy-loss straggling of low and medium energy protons on available simple materials (C, Al, Si, Ni, Cu, Zn, Ge, Se, Pd, Ag, Sb, Pt, Au, Pb) and demonstrate that the well-known Yang-O'Connor-Wang empirical formula for the energy-loss straggling of protons in matter has a clear physical interpretation. This formula predicts, on empirical grounds, energy-loss straggling values for protons that exceed the values of traditional straggling formulas (e.g., by Lindhard and Chu) at energies around 0.3 MeV/amu by a factor of 2–3. This excess is correlated to the bunching effect, which comes from the inhomogeneity feature of the electron density. Although this effect is specific to each element and can be calculated using e.g. the CasP and PASS programs, a single formula correlates better with overall experimental values. The Yang-O'Connor-Wang formula was refined accounting for subsequent experimental data.

The energy-loss straggling is sensitive to different kind of physical correlations, even in the framework of the independent electron model. According to this model the total energy loss is the sum of energy losses due to each electron $T_i(b)$, independent from the other passive electrons. Therefore, using $T(b) = \Sigma_i T_i(b)$, we get:

$$\delta\Omega^2 = N\delta x \int_0^\infty 2\pi b db \left(\sum_i \overline{T_i^2}(b) + \sum_{i \neq j} \overline{T_i}(b)\,\overline{T_j}(b) \right)$$

Equation for straggling. The first summation corresponds to the uncorrelated straggling, while the second summation (i≠j) contains the bunching or packing effects.

The first term is called uncorrelated straggling and was used in the derivation of well-known straggling formulas (Bohr, Lindhard, Chu, Bethe-Livingston, etc). The second term gives rise to bunching effects when electron i and j belong to the same atom or packing effects when electron i and j belong to the different atoms.

In this work we show that the well-known Yang-O'Connor-Wang straggling formula has captured bunching effects from the experimental data in an empirical way. This formula was further refined in this work to take into account the subsequent experimental data.

Paper reference:

On the energy-loss straggling of protons in elemental solids: The importance of electron bunching, F. F. Selau, H. Trombini, R. C. Fadanelli, M. Vos, P. L. Grande, Nuclear Inst. and Methods in Physics Research, B, 497 (2021) 70-77.

Nanoparticle-assisted radiosensitization in human glioblastoma cells exposed to high-energy photon and proton beams

Ricardo Meurer Papaléo

Metal-based nanoparticles are a promising class of new radiosensitizer agents for radiotherapy of cancer. Although a substantial amount of data has already been collected on the sensitization action of nanomaterials, results are far from being conclusive, and both, the underlying mechanisms and the role of key parameters involved in NP-enhanced radiotherapy are not fully understood. We report on radiosensitization effects produced by gold (GNP) and dextran-coated superparamagnetic iron oxide nanoparticles (SPION-DX) in human glioblastoma (GBM) cells irradiated by beams of 6 MV photons and 150 MeV H^+. The NP treatment concentration varied from 20 up to 100 µg/mL. We monitored cell viability after nanoparticle exposure alone, the actual NP uptake by the cells with ICP-MS, post-irradiation cell survival via the clonogenic assay, and DNA damage and repair by means of immunofluorescence studies with γH2AX and 53BP1. The linear-quadratic model was used to extract the α and β parameters, the α/β ratio, and the enhancement sensitization factor at 10% survival ($SER_{10\%}$).

GNP-treated cells irradiated by 6 MV-photons displayed large sensitization enhancement ratios ($SER_{10\%}$ up to 2.04). More modest effects were induced by SPION-DX, but still significant reductions in survival were achieved

(maximum $SER_{10\%}$ = 1.61). For both NPs $SER_{10\%}$ increased with the degree of metal uptake, but not necessarily with treatment concentration. The α/β ratios extracted from the survival curves are reduced by the presence of SPION-DX, but strongly increased by GNPs, suggesting that sensitization by GNPs occurs mainly via promotion of lethal complex damage, while for SPION-DX repairable damage dominates. The use of GNPs in combination with the proton beam also resulted in an increase in radiation- induced cell death, with $SER_{10\%}$ values close to 1.5. Sensitization efficacy increased linearly with GNP concentration, but not for iron oxide NPs. A general comparison of the NP action under the two types of radiation fields will be presented.

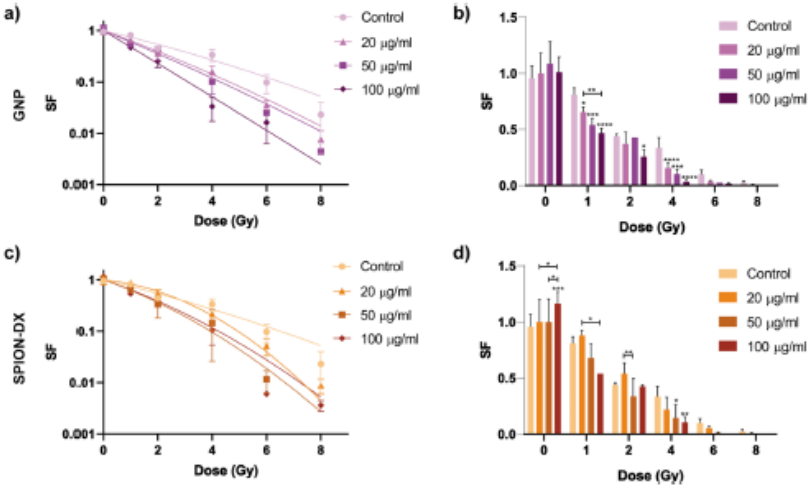

Cell survival curves as a function of dose for U87 GBM treated with GNP (a,b) and SPION-DX (c,d) at different concentrations.

Paper reference:

Intercomparison of radiosensitization induced by gold and iron oxide nanoparticles in human glioblastoma irradiated by 6 MV photons, D. B. Guerra, E. Oliveira, A.

Sonntag, P. Sbaraine, A. P. Fay, F. Morrone, R. M. Papaléo., Scientific Reports, 12 (2022) 9602.

Evidence of C migration in the SiO2 to the SiO2/Si interface of C-implanted structures

Rogerio Luis Maltez

C^+ ions at 40 keV were implanted up to 2.8 × 10^{17} cm^{-2} into SiO_2/Si(001) structures (samples kept at 600 °C) with SiO_2 thicknesses of 110, 190 and 240 nm. They were subsequently annealed at 1250 °C under a flux of 99% Ar and 1% O_2. Afterwards, we measured by Elastic Recoil Detection Analysis (ERDA) the C concentration along the whole SiO_2 until the Si side nearby the SiO_2/Si interface. We could probe C-recoiled within a narrow depth-window of about 35 nm, thus a combined procedure of ERDA and sequential etching steps of the SiO_2 cap was performed. After each etching step, which removed ~ 30 nm of the oxide, we calculated a normalized result, both in extension and in intensity (in relation to a standard sample). The C distribution profile for the 110 nm case is consistent with the SRIM (The Stopping and Range of Ions in Matter) simulation of implanted C into a SiO_2(110-nm)/SiC(55-nm)/Si(bulk) structure. For the 190 nm one, the measured C shows a shift of ~ 40 nm towards SiO_2/Si interface and a systematic concentration-increase from about the middle of the cap layer up to the SiO_2/Si interface. However, according to SRIM simulation, the C concentration was supposed to decrease when approaching the interface. For the 240 nm SiO_2-cap, it shows a peak-

shift of ~ 50 nm towards the SiO_2/Si interface in relation to the simulation. Our results indicate that the SiO_2/Si interface efficiently attracts C within a capture range of about 50 nm from the interface. This C peak-shift in the SiO_2 towards the SiO_2/Si interface, is only consistent with diffusion models based on C dissolved in SiO_2, forming bonds with Si or O, or even C-C complexes, but not with SiC precipitation in it.

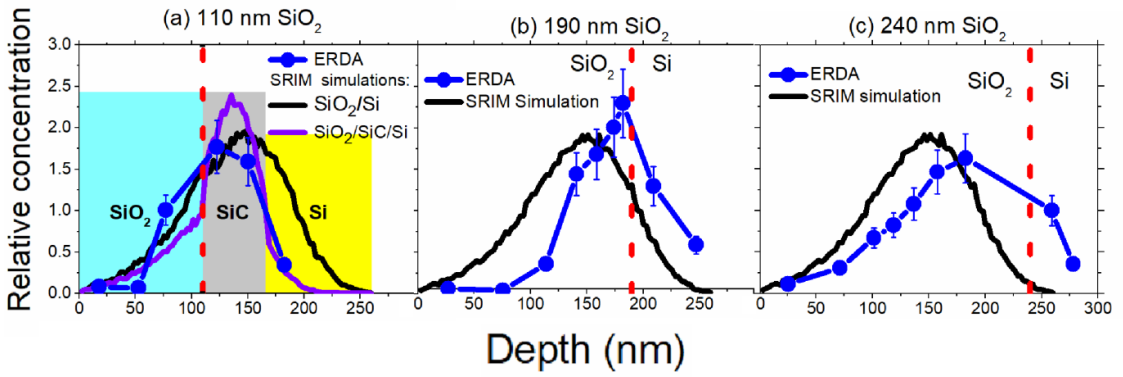

Full blue circles connected by blue lines are the carbon depth-distribution in the SiO_2 layers (up to the Si side underneath the interface) obtained by ERDA measurements for the samples with SiO_2-cap thickness of: (a) 110 nm, (b) 190 nm and (c) 240 nm. They represent the ratio of areas (relative to a reference sample) in a depth-window of about 35 nm and after etching steps, which removes about 30 nm of the SiO_2. The vertical red dashed lines locate the SiO_2/Si interface positions for each case. The SRIM continuous black-lin, which is present in all figures, is the deep-distribution profile that simulates C implantation into the precursor SiO_2/Si(bulk). In (a) is an additional SRIM deep-distribution profile (the continuous purple-line) that simulates C implantation into the SiO_2(110-nm)/SiC(55-nm)/Si(bulk) layered structure. This is the final synthesized structure.

Paper reference:

Evidence of C migration in the SiO_2 to the SiO_2/Si interface of C-implanted structures, E. Ribas, R. L. Maltez, Thin Solid Films, 730 (2021) initial 138702-138709.

Synthesis and characterization of silver nanoparticles using a green chemistry approach

Silma Alberton Corrêa

The application of H_2 as a clean and renewable source of energy can play a significant role towards a more sustainable resource to fulfill the future energy demands of the world. In order to obtain H_2 from water splitting using light as excitation source, a semiconductor-based material with appropriate properties to catalyze such reaction is required. Furthermore, an enhanced photocatalytic activity can be achieved by the addition of co-catalysts, such as noble metal nanoparticles (NPs). Therefore, there is a current demand for environment-friendly methods, using non-toxic chemicals to synthesize these materials. In this context, microwave (MW) assisted aqueous synthesis represents an alternative that follows green chemistry approaches and that could lead to faster and less expensive procedures than the ones generally used. In this work we used glycerol and starch in a MW assisted synthesis of silver nanoparticles (Ag NPs). The nanoparticles obtained were impregnated into commercial TiO2 NPs (AEROXIDE® TiO2-P25) and tested for the H_2 evolution in the photo-reform of methanol at room temperature. Samples were characterized by UV–vis spectroscopy, X-ray diffraction (XRD), transmission electron microscopy (TEM), UV-Vis diffuse reflectance spectroscopy (UV-Vis DRS), and Rutherford Backscattering Spectrometry (RBS). The elemental composition was determined by fitting of the RBS data using the SIMNRA software.

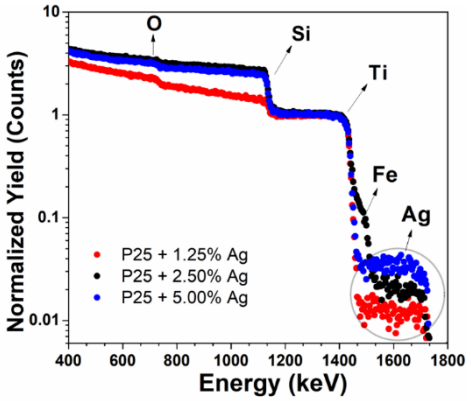

Fig. 1: RBS analysis of the TiO_2@AgNPs impregnated with different amounts of Ag, which is shown in the figure as Ag/TiO_2 wt.%. The silicon signal in all three samples stands for the substrate on which solutions of the TiO_2@AgNPs were dripped.

RBS results revealed that the Ag/TiO2 wt. % amount that were impregnated in the TiO2 was less than 30% of the amounts in the corresponding Ag NPs suspension. For the 1.25, 2.5 and 5.00% samples, the amounts determined by RBS were 0.34, 0.62 and 1.02, respectively. Besides, there is a clear signal of iron (Fe) in the P25 + 2.50% Ag sample, that we attributed to a contamination during the impregnation procedure. Photocatalytic tests using these TiO2@AgNPs samples under UV-Vis irradiation in the presence of methanol-water solutions showed that the H2 generation rate was much higher compared with the amounts produced using pure TiO2 NPs. Moreover, the H2 generation is proportional to the amount of Ag NPs loaded onto the TiO2 NPs.

Paper reference:

Microwave assisted synthesis of silver nanoparticles and its application in sustainable photocatalytic hydrogen evolution, G. B. Strapasson, M. Assis, C. W. Backes, S. A. Corrêa, E. Longo, and D. E. Weibel, International Journal of Hydrogen Energy, 46 (2021)34264-34275.

Publications in peer reviewed journals

[1] Bolzan, C. A., Manzo, D. J., Notthoff, C., Kluth, P., & Giulian, R. (2021). Stoichiometry-dependent porosity by ion irradiation: In (1–x) Al (x) Sb films. **Journal of Physics and Chemistry of Solids**, 148, 109769.

[2] Bolzan, C. A., Johannessen, B., Wu, Z., & Giulian, R. (2021). Local and extended atomic structure of strained polycrystalline In (1-x) Al (x) Sb alloys. **Journal of Physics and Chemistry of Solids**, 150, 109844.

[3] Ullah, H., Rahman, A. U., Aragão, E. L., Barbosa, F. F. A., Pergher, K. G. R., Giulian, R., ... & Khan, S. (2021). Homogeneous V incorporation via single-step anodization: structural doping or heterostructure formation?. **Applied Surface Science**, 556, 149694.

[4] Bolzan, C. A., Johannessen, B., Wu, Z., & Giulian, R. (2021). Local structure of porous InSb films: From first to third-shell EXAFS investigation. **Solid State Sciences**, 119, 106705.

[5] Tee, B. P. E., Vos, M., Trombini, H., Selau, F. F., Grande, P. L., & Thomaz, R. (2021). The influence of radiation damage on electrons and ion scattering measurements from PVC films. **Radiation Physics and Chemistry**, 179, 109173.

[6] Selau, F. F., Trombini, H., Fadanelli, R. C., Vos, M., & Grande, P. L. (2021). On the energy-loss straggling of protons in elemental solids: The importance of electron bunching. **Nuclear Instruments and Methods in Physics Research Section B: Beam Interactions with Materials and Atoms**, 497, 70-77.

[7] Creutzburg, S., Niggas, A., Weichselbaum, D., Grande, P. L., Aumayr, F., & Wilhelm, R. A. (2021). Angle-dependent charge exchange and energy loss of slow highly charged ions in freestanding graphene. **Physical Review A**, 104(4), 042806.

[8] Grande, P. L. (2021). Bohr's stopping-power formula derived for a classical free-electron gas. **Physical Review A**, 104(1), 012807.

[9] Alencar, I., Hatori, M., Marmitt, G. G., Trombini, H., Grande, P. L., Dias, J. F., Papaléo, R. M., Mücklich, A., Assmann, W., Toulemonde, M. & Trautmann, C. (2021). Nanoparticle emission by electronic sputtering of CaF2 single crystals. **Applied Surface Science**, 537, 147821.

[10] Megginson, R., Grillo, F., Francis, S. M., Paes, V. Z. C., Trombini, H., Grande, P. L., Rossall, A. K., van den Berg, J.A. & Baddeley, C. J. (2022). Thermal behaviour of Cu and Au nanoparticles grown on CeO2 thin films. **Applied Surface Science**, 575, 151656.

[11] Niggas, A., Creutzburg, S., Schwestka, J., Wöckinger, B., Gupta, T., Grande, P. L., Dominik, E., Marques, J. P., Bayer, B. C., Aumayr, F., Bennett, R. & Wilhelm, R. A. (2021). Peeling graphite layer by layer reveals the charge exchange dynamics of ions inside a solid. **Communications Physics**, 4(1), 180.

[12] Creutzburg, S., Mergl, M., Hübner, R., Jirka, I., Erb, D., Heller, R., Niggas, A., Grande, P. L., Aumayr, F., Wilhelm, R. A., Kalbac, M., & Facsko, S. (2021). Fluorination of graphene leads to susceptibility for nanopore formation by highly charged ion impact. **Physical Review Materials**, 5(7), 074007.

[13] Alencar, I., Silva, M. R., Leal, R., Grande, P. L., & Papaléo, R. M. (2021). Impact features induced by single fast ions of different charge-state on muscovite mica. **Atoms**, 9(1), 17.

[14] Bunk, K., Alencar, I., Morgenroth, W., Bertram, F., Schmidt, C., Zimmer, D., Gruszka, P., Hanefeld, M., Bayarjargal, L., Trautmann, C. & Winkler, B. (2021). Surface and subsurface damage in 14 MeV Au ion-irradiated diamond. **Journal of Applied Physics**, 130(10), 105303.

[15] da Rosa, C. T. W., da Silva, J. C. D. R., Dias, J. F., & Locatelli, A. (2021). Proposta para abordagem de tópicos de Física Nuclear no ensino médio: análise de atividades com professores de Física em formação inicial. **Caderno Brasileiro de Ensino de Física**, 38(1), 513-537.

[16] Romolo, F. S., Sarilar, M., Antoine, J., Mestria, S., Rossi, S. S., Gallidabino, M. D., de Souza, G. M. S., Chytry, P. & Dias, J. F. (2021). Ion beam analysis (IBA) and instrumental neutron activation analysis (INAA) for forensic characterisation of authentic Viagra® and of sildenafil-based illegal products. **Talanta**, 224, 121829.

[17] de Souza, M. R., Garcia, A. L. H., Dalberto, D., Martins, G., Picinini, J., de Souza, G. M. S., Chytry, P., Dias, J. F., Bobermin, L. D., Quincozes-

Santos, A. & da Silva, J. (2021). Environmental exposure to mineral coal and by-products: Influence on human health and genomic instability. **Environmental Pollution**, 287, 117346.

[18] Dalberto, D., Nicolau, C. C., Rosa De Sousa, M., Garcia, A. L. H., Boaretto, F., Picada, J. N., de Souza, G. M. S., Chytry, P., Dias, J. F., Feistel, C. C., Ferraz, A. B. F., Grivicich, I. & Da Silva, J. (2021). Genotoxic effect induced by dried nicotiana tabacum leaves from tobacco barns (kiln-houses) in chinese hamster lung fibroblast cells (V79). **Journal of Toxicology and Environmental Health, Part A**, 84(17), 689-701.

[19] Selbach, M. T., Scotti, A. S., Feistel, C. C., Nicolau, C. C., Dalberto, D., Dos Santos, N. G., Borsoi, G., Ferraz, A. B. F., Grivicich, I., de Souza, G. M. S., Chytry, P., Dias, J. F., Corrêa, D. S. & da Silva, J. (2021). Evaluation of the cytotoxic and genotoxic effects of Sida planicaulis Cav extract using human neuroblastoma cell line SH-SY5Y. **Journal of Toxicology and Environmental Health, Part A**, 84(8), 345-355.

[20] de Souza, M. R., Garcia, A. L. H., Dalberto, D., Nicolau, C., Gazzineu, A. L., Grivicich, I., Boaretto, F. Picada, J. N., de Souza, G. M. S., Chytry, P., Dias, J F., D. S. Corrêa & da Silva, J. (2021). Evaluation of soils under the influence of coal mining and a thermoelectric plant in the city of Candiota and vicinity, Brazil. **Mutation Research/Genetic Toxicology and Environmental Mutagenesis**, 866, 503350.

[21] Debastiani, R., Dos Santos, C. E. I., & Dias, J. F. (2021). Elemental characterization of sparkling wine and cork stoppers. **Current research in food science**, 4, 670-678.

[22] Debastiani, R., dos Santos, C. E. I., Ramos, M. M., Souza, V. S., Yoneama, M. L., Amaral, L., & Dias, J. F. (2021). Elemental concentration of tomato paste and respective packages through particle-induced X-ray emission. **Journal of Food Composition and Analysis**, 97, 103770.

[23] Debastiani, R., dos Santos, C. E. I., Ramos, M. M., Souza, V. S., Amaral, L., & Dias, J. F. (2021). Variance of elemental concentrations of organic products: the case of Brazilian coffee. **Nuclear Instruments and Methods in Physics Research Section B: Beam Interactions with Materials and Atoms**, 486, 18-21.

[24] Quintana-Sosa, M., León-Mejía, G., Luna-Carrascal, J., Rodríguez, I. L., Acosta-Hoyos, A., Anaya-Romero, M., Trindade, C., Narváez, D. M., de Restrepo, H. G., Dias, J. F., Niekraszewicz, L., Garcia, A. L. H., Rohr, P., da Silva, J. & Henriques, J. A. P. (2021). Cytokinesis-block micronucleus cytome (CBMN-CYT) assay biomarkers and telomere length analysis in relation to inorganic elements in individuals exposed to welding fumes. **Ecotoxicology and Environmental Safety**, 212, 111935.

[25] Neto, J. L. S., de Carli, R. F., Lehmann, M., de Souza, C. T., Niekraszewicz, L. A. B., Dias, J. F., da Silva, F. R., da Silva, J. & Dihl, R. R. (2022). In vivo and in silico approaches to assess surface water genotoxicity from Tocantins River, in the cities of Porto Nacional and Palmas, Brazil. J**ournal of Environmental Science and Health**, Part C, 40(1), 27-45.

[26] Chytry, P., Souza, G. M. S. D., Debastiani, R., Dos Santos, C. E. I., Antoine, J. M., Banas, A., Calcagnile, L., Chiari, M., Hajdas, I., Molnar, M., Pelicon, P., Barradas, N. P., Quarta, G., Romolo, F. S., Simon, A. & Dias, J. F. (2022). The potential of accelerator-based techniques as an analytical tool for forensics: The case of coffee. **Forensic Science International**, 335, 111281.

[27] Giulian, R., Bolzan, C. A., Rossetto, L. T., de Andrade, A. M. H., & Dias, J. F. (2022). In1-xGaxSb nanofoams made by ion irradiation of sputtered films: Atomic composition and structure. **Thin Solid Films**, 753, 139263.

[28] Jobim, P. F. C., Iochims dos Santos, C. E., Dias, J. F., Kelemen, M., Pelicon, P., Mikuš, K. V., Pascolo, L., Gianoncelli, A., Bedolla, D. E. & Rasia-Filho, A. A. (2023). Human Neocortex Layer Features Evaluated by PIXE, STIM, and STXM Techniques. **Biological Trace Element Research**, 201(2), 592-602.

[29] Picinini, J., Oliveira, R. F., Garcia, A. L. H., da Silva, G. N., Sebben, V. C., de Souza, G. M. S., Dias, J. F., Corrêa, D. S. & da Silva, J. (2022). In vitro genotoxic and mutagenic effects of water samples from Sapucaia and Esteio streams (Brazil) under the influence of different anthropogenic activities. **Mutation Research/Genetic Toxicology and Environmental Mutagenesis**, 878, 503484.

[30] Quarta, G., Hajdas, I., Molnár, M., Varga, T., Calcagnile, L., D'Elia, M., Molnar, A.& Jull, A. J. T. (2022). The IAEA Forensics Program: Results of the AMS 14C Intercomparison Exercise on Contemporary Wines and Coffees. **Radiocarbon**, 64(6), 1513-1524.

[31] de Vila Bauer, D., Debastiani, R., Telles de Souza, C., Amaral, L., & Ferraz Dias, J. (2022). The potentialities of ultrasound as an alternative to chemical etching for proton beam writing micropatterning. **Journal of Applied Polymer Science**, 139(25), e52407.

[32] Lourenço, N. A., Hoff, G., Borba, I., de Pires, M. M., do Nascimento, C. D. D., Souza, E. G., Garcia, T. S., Trombini, H. & Pereira, L. G. (2021). Uso do Método de Monte Carlo para caracterização adicional de materiais para aplicação em blindagem de fótons. **Revista Brasileira de Física Médica**, 15, 610-610.

[33] Gutierres, L. I., Migowski, P., Alencar, I., Thomaz, R. S., & Feil, A. F. (2021). Photocurrent improvement from magnetron DC sputtered and thermally treated ruthenium-based catalyst decoration onto BiVO4 photoanodes. **Nuclear Instruments and Methods in Physics Research Section B: Beam Interactions with Materials and Atoms**, 494, 10-15.

[34] Thomaz, R., Lima, N. W., Teixeira, D., Gutierres, L. I., Alencar, I., Trautmann, C., Grande, P. L. & Papaléo, R. M. (2021). Ion tracks in ultrathin polymer films: The role of the substrate. **Current Applied Physics**, 32, 91-97.

[35] Thomaz, R. S., Ernst, P., Grande, P. L., Schleberger, M., & Papaléo, R. M. (2022). Cratering Induced by Slow Highly Charged Ions on Ultrathin PMMA Films. **Atoms**, 10(4), 96.

[36] Patta, P. C., de Oliveira, E. M. N., de Goulart, A. C. F., Zaluski, A. B., Papaléo, R. M., & Vianna, M. R. M. (2022). Amyloid-β 42 oligomeric forms: AFM nanoscale structural characterization and impact on long-term memory of young and aged zebrafish. **Neuroscience**. 10;497:271-281.

[37] Nikolskaya, A., Okulich, E., Korolev, D., Stepanov, A., Nikolichev, D., Mikhaylov, A., Tetelbaum, D., Aleksei Almaev, A., Bolzan, C. A., Antônio Buaczik, A., Giulian, R., Grande, P. L., Kumar, A., Kumar, M. & Gogova, D.

(2021). Ion implantation in β-Ga2O3: Physics and technology. **Journal of Vacuum Science & Technology A: Vacuum, Surfaces, and Films**, 39(3), 030802.

[38] Feijó, T. O., Copetti, G., Gerling, E. R. F., Hanke, M., Lopes, J. M. J., Radtke, C., & Soares, G. V. (2021). The role of substrate on the growth of 2D heterostructures by CVD. **Applied Surface Science**, 539, 148226.

[39] Leal da Silva, E., Cuña, A., Cadorin, M., Marcuzzo, J. S., Radtke, C., Baldan, M. R., Rodrigues-Siqueli, A. C., & de Fraga Malfatti, C. (2022). Influence of the support and SnO 2 content on the electrocatalytic properties of PdSn/C electrocatalysts for EOR in alkaline medium. **Waste and Biomass Valorization**, 1-12.

[40] Moreno, Y. P., da Silva, W. L., Stedile, F. C., Radtke, C., & dos Santos, J. H. (2021). Micro and nanodomains on structured silica/titania photocatalysts surface evaluated in RhB degradation: Effect of structural properties on catalytic efficiency. **Applied Surface Science Advances**, 3, 100055.

[41] Valente, R. C., Falqueto, J. B., Bocchi, N., Maltez, R. L., & Dick, L. F. (2021). Analysis of anodic nanotubular oxide on homogeneous Ti-Si alloys for Li-ion battery anodes. **Journal of Alloys and Compounds**, 888, 161659.

[42] Ribas, E., & Maltez, R. L. (2021). Evidence of C migration in the SiO2 to the SiO2/Si interface of C-implanted structures. **Thin Solid Films**, 730, 138702.

[43] Strapasson, G. B., Assis, M., Backes, C. W., Corrêa, S. A., Longo, E., & Weibel, D. E. (2021). Microwave assisted synthesis of silver nanoparticles and its application in sustainable photocatalytic hydrogen evolution. **International Journal of Hydrogen Energy**, 46(69), 34264-34275.

[44] Pitthan, E., Moro, M. V., Correa, S. A., & Primetzhofer, D. (2021). Assessing boron quantification and depth profiling of different boride materials using ion beams. **Surface and Coatings Technology**, 417, 127188.

[45] Castegnaro, M. V., Gorgeski, A., Alves, M. C., & Morais, J. (2021). Carbon supported Pd–Cu nanoalloys: support and valence band structure influence on reduction and oxidation reactions. **Nanoscale Advances**, 3(21), 6138-6143.

[46] de Oliveira, F. S., Nogueira, M. J., Fabrim, Z. E., & Fichtner, P. F. (2021). Electron irradiation effects in Au thin films. **Journal of Materials Science: Materials in Electronics**, 32(10), 13291-13304.

[47] Konrad, B., Fabrim, Z. E., Timm, M. M., & Fichtner, P. F. (2021). Electron irradiation effects on Ag nanoparticles. **Journal of Materials Science**, 56(13), 8202-8208.

[48] Timm, M. D. M., Oliviero, E., Sun, W., Gomes, S., Hamaoui, G., Fichtner, P. F. P., & Frety, N. (2022). Ion implantation effects on the microstructure, electrical resistivity and thermal conductivity of amorphous CrSi 2 thin films. **Journal of Materials Science**, 1-12.

[49] Figueiredo, W. T., Prakash, R., Vieira, C. G., Lima, D. S., Carvalho, V. E., Soares, E. A., Buchner, S., Raschke, H., Perez-Lopez, O. W., Baptista, D. L., Hergenröder, R., Segala, M. & Bernardi, F. (2022). New insights on the electronic factor of the SMSI effect in Pd/TiO2 nanoparticles. **Applied Surface Science**, 574, 151647.

[50] Qadir, M. I., Baptista, D. L., & Dupont, J. (2022). Effect of Support Nature on Ruthenium-Catalyzed Allylic Oxidation of Cycloalkenes. **Catalysis Letters**, 1-8.

[51] Qadir, M. I., Albo, J., de Pedro, I., Cieslar, M., Hernández, I., Brüner, P., Grehl, T., Castegnaro, M. V., Morais, J., Martins, P. R., Silva, C. G., Nisar, M. & Dupont, J. (2022). Nanoarchitectonics of CuNi bimetallic nanoparticles in ionic liquids for LED-assisted synergistic CO2 photoreduction. **Molecular Catalysis**, 531, 112654.

[52] Padilha Fontoura, C., Dotta Maddalozzo, A. E., Machado Rodrigues, M., Barbieri, R. A., da Silva Crespo, J., Figueroa, C. A., & Aguzzoli, C. (2021). Nitrogen Incorporation into Ta Thin Films Deposited over Ti6Al4V: A Detailed Material and Surface Characterization. **Journal of Materials Engineering and Performance**, 30(6), 4094-4102.

[53] Santos, P. B., Baldin, E. K., Krieger, D. A., de Castro, V. V., Aguzzoli, C., Fonseca, J. C., Rodrigues, M., Lopes, M. A. & de Fraga Malfatti, C. (2021). Wear performance and osteogenic differentiation behavior of plasma electrolytic oxidation coatings on Ti-6Al-4V alloys: Potential application for bone tissue repairs. **Surface and Coatings Technology**, 417, 127179.

[54] Cruz, R. L., Nascimento, C. D., Souza, E. G., Aguzzoli, C., Moraes, A. C. B. K., & Lund, R. G. (2022). On the Adhesion of Protein in Nitrided Metallic Coatings for Electrosurgical Electrodes of Stainless Steel. **Materials Research**, 25.

[55] Baldin, E. K., Santos, P. B., de Castro, V. V., Aguzzoli, C., Maurmann, N., Girón, J., Pranke, P. & Malfatti, C. D. F. (2022). Plasma Electrolytic Oxidation (PEO) Coated CP-Ti: Wear Performance on Reciprocating Mode and Chondrogenic–Osteogenic Differentiation. **Journal of Bio-and Tribo-Corrosion**, 8, 1-16.

Books and books chapters

Title: Model dielectric functions for ion stopping: The relation between their shell corrections, plasmon dispersion and Compton profiles.
Authors: Maarten Vos e Pedro Luis Grande Ano: 2022.
Publishing company: Academic Press Modo de acesso: https://ftp.math.utah.edu/pub/tex/bib/toc/advquantumchem.html#5():2022
ISSN (print): 9780323991889
ISNN (online): 9780323991896

Title: Reliability and Comparison of Some GEANT4-DNA Processes and Models for Proton Transportation: An Ultra-Thin Layer Study.
Authors: Gabriela Hoff; Raquel S. Thomaz; Leandro I. Gutierres; Sven Muller; Viviana Fanti; Elaine Streck; Ricardo M. Papaléo.
Publishing company: IntechOpen
Modo de acesso: https://www.intechopen.com/books/11066
ISSN (print): 978-1-83968-759-4
ISNN (online): 978-1-83968-761-7

Title: Desempeño fotoeletroquímico de nanoestructuras de niobio obtenidas por anodización: efecto de la concentración de glicerol.

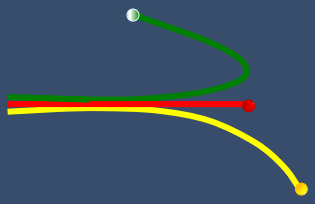

Laboratório de Implantação Iônica
Instituto de Física – UFRGS

Ion Implantation Laboratory
Institute of Physics - UFRGS

Biennial Report 2021/22

Authors: Janice Adamski; Leonardo Marasca Antonini; Melisa Olivera; Cesar Aguzzoli; Roberto Hübler; Andrea De León; Juan Bussi; Célia de Fraga Malfatti.

Publishing company: Brazilian Journals

Modo de acesso: doi.org/10.35587/brj.ed.0000987

ISNN (online): 978-65-86230-78-9

Oral Contributions and Invited Talks

Dheryck Schwendler Cabeda, Oral Contribution, MRS Spring Meeting. "WS2 Films Obtained with a Low Thermal Budget Sulfurization Process". 2021, evento online.

Paulo Fernando Papaleo Fichtner, Oral Contribution, 22nd International Conference on Ion Beam Modification of Materials. "Elastic electron scattering experiments: an alternative to light ion irradiation". 2022, Lisbon-Portugal.

Mariana Timm, Oral Contribution, 22nd International Conference on Ion Beam Modification of Materials. "Influence of dpa Rate on Carbide Precipitation and Ar Bubble Growth in AISI 316L Alloys Irradiated with Au and Ag Ions". 2022, Lisbon-Portugal.

Bárbara Konrad, Oral Contribution, 22nd International Conference on Ion Beam Modification of Materials. "Coarsening of Embedded Ag nanoparticles under Ne+ ion irradiation". 2022, Lisbon-Portugal.

Bárbara Konrad, Oral Contribution, SBPMat. "Coarsening of Embedded Ag nanoparticles under Ne+ ion irradiation". 2022, Foz do Iguaçu.

Franciele Silva Mendes de Oliveira, Oral Contribution, X Conferencia Latinoamericana de Colisiones Inelásticas en la Materia (CLACIM).

"Elastic and inelastic electron scattering experiments on shape evolution of Au and CdSe thin films". 2022, Salta.

Johnny Ferraz Dias, Invited Talk, X Conferência Latinoamericana de Colisiones Inelásticas en la Materia (CLACIM). "Seções de choque de produção de raios X da camada K de Ti, Cr, Ni e Zn induzidas por íons de cloro". 2022, Salta.

Henrique Trombini, Oral Contribution, X Conferência Latinoamericana de Colisiones Inelásticas en la Materia (CLACIM). "Structural characterization of a Pt ultra-thin films by electron and ion based". 2022, Salta.

Henrique Trombini, Invited Talk, X High Resolution Depth Profiling Conference. "MEIS technique and PowerMEIS3 code: a powerful combination for material analysis". 2022, Adelaide.

Taiane Neves, Oral presentation, 35th Symposium on Microelectronics Technology and Devices, "The influence of crosslinker concentration on PVA insulation characteristics" 2021, Virtual Event.

Igor Alencar, Oral Contribution, International Conference on Ion Beam Analysis / Particle Induced X-ray Emission & Secondary Ion Mass Spectrometry. "Operating a dual-stage mirror ToF-MeV-SIMS instrument with continuous sources of primary ions: Optimization and possibilities". 2021, Online Event.

Igor Alencar, Oral Contribution, XX Brazilian Material Research Society Meeting. "Paleo-detectors: Could Rock Salt passive and indirectly detect neutrinos?". 2022, Foz do Iguaçu.

Pedro Luis Grande, Oral Contribution, Non-linear ion stopping calculations for a classical free-electron gas, 9th international conference on atomic collisions in solids & 11th international symposium on swift heavy ions in matter, Junho 19-24, Helsinki, 2022.

Supervision of Thesis and Dissertations (completed)

Matheus Ramos Caloni. "Avaliação da biodistribuição elementar em larvas de peixe-zebra expostas a nanopartículas de óxido de ferro". Pontifícia Universidade Católica do Rio Grande do Sul. Engenharia e Tecnologia de Materiais. Orientador: Prof. Dr. Ricardo Papaléo. 2021.

Angelika von Schmude. "Efeitos da radiação ionizante em nanopartículas magnéticas de óxido de ferro". Pontifícia Universidade Católica do Rio Grande do Sul. Engenharia e Tecnologia de Materiais. Orientador: Prof. Dr. Ricardo Papaléo. 2021.

Dheryck Schwendler Cabeda. "Sulfurização de filmes de WO3 visando à obtenção do material semicondutor bidimensional WS2". Universidade Federal do Rio Grande do Sul. Instituto de Informática. Programa de Pós-Graduação em Microeletrônica. Orientador: Cláudio Radtke. 2021.

Leandro Tedesco Rosseto. "Dispositivo para análise e caracterização de materiais semicondutores utilizados como sensores de gás". Universidade Federal do Rio Grande do Sul. Programa de Pós-Graduação em Ciências dos Materias. Orientadora: Raquel Giulian. Coorientador: Livio Amaral. 2021.

Henrique Bauermann Fonteles. “Imageamento e Análise de Células U87 tratadas com cisplatina por micro-PIXE”. Universidade Federal do Rio Grande do Sul. Instituto de Física. Programa de Pós-Graduação em Física. Orientador: Prof. Dr. Pedro Luis Grande. 2022.

Paola Chytry. “Preparação e caracterização de filmes poliméricos para utilização em espectrometria de massa por tempo de voo”. Universidade

Federal do Rio Grande do Sul. Programa de Pós-Graduação em Ciências dos Materias. Orientador: Prof. Dr. Johnny Ferraz Dias. 2022.

Gabriel Justen Dapper. "Desenvolvimento de um dispositivo inovador de simulação dinâmica do sistema respiratório para avaliação de um TNT revestido com filme de Cu". Orientador: Cesar Aguzzoli. Coorientador: Carlos Alejandro Figueroa. 2022.

Ricardo Augusto Zanotto Razera. “Células Solares de Perovskita Híbridas: Análise de Desempenho e estabilidade em polarização reversa”. Universidade Federal do Rio Grande do Sul. Instituto de Informática. Programa de Pós-Graduação em Microeletrônica. Orientador: Prof. Dr. Henri Ivanov Boudinov. 2021.

Ítalo Martins Oyarzabal. “Efeitos da Implantação de Ar e da irradiação de Au sobre a microestrutura do aço AISI 316L para aplicações nucleares”. Universidade Federal do Rio Grande do Sul. Instituto de Física. Programa de Pós-Graduação em Física. Orientador: Prof. Dr. Paulo Fernando Papaleo Fichtner. 2021.

Felipe Ferreira Selau. “Poder de freamento e dispersão da perda de energia de prótons em filmes finos de platina: a importância do agrupamento de elétrons”. Universidade Federal do Rio Grande do Sul. Instituto de Física. Programa de Pós-Graduação em Física. Orientador: Prof. Dr. Pedro Luis Grande Coorientador: Prof. Dr. Jonder Morais. 2021.

Danieli Born Guerra. "Nanoparticles for radiation therapy enhancement: investigation of radiosensitization induced by gold and iron oxide nanoparticles in glioblastoma cells exposed to photon and proton beams". Pontifícia Universidade Católica do Rio Grande do Sul. Engenharia e Tecnologia de Materiais. Orientador: Prof. Dr. Ricardo Papaléo. 2021.

Patent

Registry number: BR 10 2014 008755 9. **Holder:** Fundação Universidade de Caxias do Sul.

Invention title: Filme bactericida, processo de preparação do mesmo e método de tratamento de efluente.

Inventors: F. Zarpelon, M. Giovanela, J. S. Crespo, C. Aguzzoli.

Deposit date: 10/04/2014; **Publication Date:** 01/12/2015; **Concession date:** 19/01/2021.

Members in International Committees and in Editorial Boards

Fernanda Chiarello Stedile - Member of the international committee of the International Conference on Ion Beam Analysis (IBA).

Johnny Ferraz Dias - Member of the International Committee of the International Conference on Particle-Induced X-ray Emission (PIXE).

Johnny Ferraz Dias - Member of the International Committee of the International Symposium on BioPIXE (BioPIXE).

Paulo F. P. Fichtner - Member of the International Committee of the Conference on Ion Beam Modification of Materials (IBMM).

Paulo F. P. Fichtner - Member of the Physics Committee from the Brazilian National Research Council (CNPq).

Pedro L. Grande - Member of the international committee of the International Conference on Ion Beam Analysis (IBA).

Pedro L. Grande - Member of the international committee of the International Conference of Atomic Collision in Solids (ICACS).

Pedro L. Grande - Member of the international committee of the International Workshop on High-Resolution Depth Profiling (HRDP)

Pedro L. Grande - Member of the International Committee of Colisiones Inelasticas na Materia.

R. M. Papaléo - Member of the International Committee of the conference Radiation Effects on Insulators.

R. M. Papaléo - Member of the International Committee of the International Symposium on Swift Heavy Ions in Matter.

Funding programs and agencies

Instituto Nacional de Engenharia de Superfícies

INES

http://engenhariadesuperficies.com.br/

Finep
FINANCIADORA DE INOVAÇÃO E PESQUISA

FINEP

http://www.finep.gov.br/

PRONEX – Programa de Apoio aos Núcleos de Excelência

http://www.cnpq.br/web/guest/pronex

CNPq

http://cnpq.br/

CAPES

CAPES

http://www.capes.gov.br/

Laboratório de Implantação Iônica
Instituto de Física
Universidade Federal do Rio Grande do Sul

Av. Bento Gonçalves 9500
91501-970, Porto Alegre – RS, Brazil
Phone +55 51 33087004
Fax +55 51 33087296
http://implantador.if.ufrgs.br